

Attenuation

The attenuation or transmission loss of optical fibers has proved to be one of the most important factors in bringing about their wide acceptance in telecommunications. As channel attenuation largely determined the maximum transmission distance prior to signal restoration, optical fiber communications became especially attractive when the transmission losses of fibers were reduced below those of the competing metallic conductors (less than 5 dB km^{-1}). Signal attenuation within optical fibers, as with metallic conductors, is usually expressed in the logarithmic unit of the decibel. The decibel, which is used for comparing two power levels, may be defined for a particular optical wavelength as the ratio of the input (transmitted) optical power P_i into a fiber to the output (received) optical power P_o from the fiber as:

$$\text{Number of decibels (dB)} = 10 \log_{10} \frac{P_i}{P_o} \quad (2.1)$$

This logarithmic unit has the advantage that the operations of multiplication and division reduce to addition and subtraction, while powers and roots reduce to multiplication and division. However, addition and subtraction require a conversion to numerical values which may be obtained using the relationship:

$$\frac{P_i}{P_o} = 10^{(\text{dB}/10)} \quad (2.2)$$

In optical fiber communications the attenuation is usually expressed in decibels per unit length (i.e. dB km^{-1}) following:

$$\alpha_{\text{dB}} L = 10 \log_{10} \frac{P_i}{P_o} \quad (2.3)$$

where α_{dB} is the signal attenuation per unit length in decibels which is also referred to as the fiber loss parameter and L is the fiber length. A number of

mechanisms are responsible for the signal attenuation within optical fibers. These mechanisms are influenced by the material composition, the preparation and purification technique, and the waveguide structure. They may be categorized within several major areas which include material absorption, material scattering (linear and nonlinear scattering), curve and microbending losses, mode coupling radiation losses and losses due to leaky modes.

Material Absorption Losses in Silica Glass Fibers

Material absorption is a loss mechanism related to the material composition and the fabrication process for the fiber, which results in the dissipation of some of the transmitted optical power as heat in the waveguide. The absorption of the light may be intrinsic (caused by the interaction with one or more of the major components of the glass) or extrinsic (caused by impurities within the glass).

1. Intrinsic Absorption

An absolutely pure silicate glass has little intrinsic absorption due to its basic material structure in the near-infrared region. However, it does have two major intrinsic absorption mechanisms at optical wavelengths which leave a low intrinsic absorption window over the 0.8 to 1.7 μm wavelength range, as illustrated in Figure 2.1, which shows a possible optical attenuation against wavelength characteristic for absolutely pure glass.

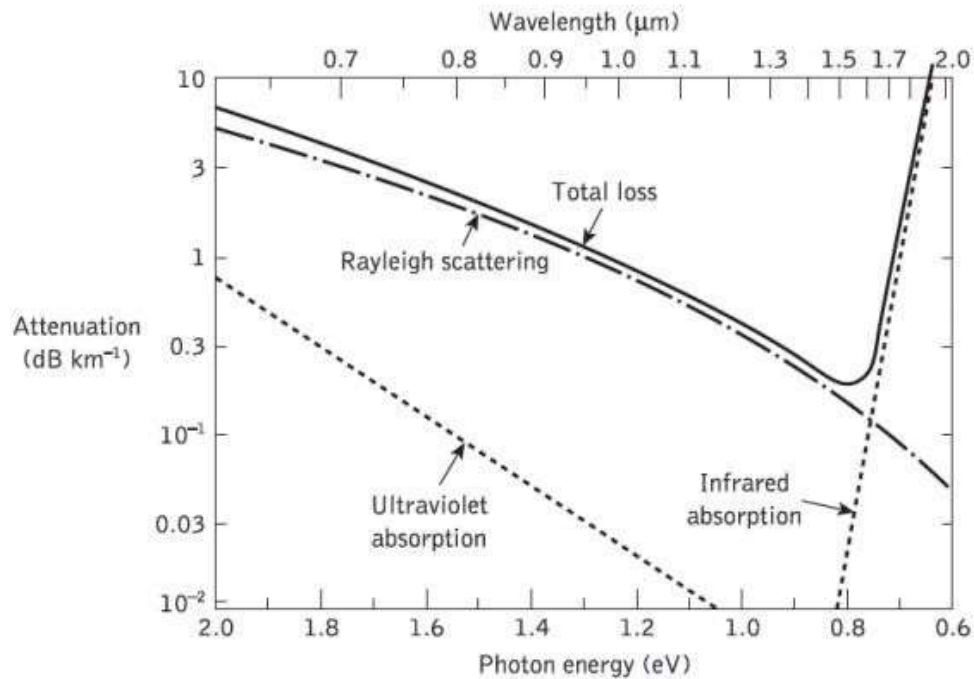


Figure 2.1 The attenuation spectra for the intrinsic loss mechanisms in pure GeO₂-SiO₂ glass

[Source: <http://img.brainkart.com>]

It may be observed that there is a fundamental absorption edge, the peaks of which are centered in the ultraviolet wavelength region. This is due to the stimulation of electron transitions within the glass by higher energy excitations. The tail of this peak may extend into the window region at the shorter wavelengths, as illustrated in Figure 2.1. Also in the infrared and far infrared, normally at wavelengths above 7 μm, fundamentals of absorption bands from the interaction of photons with molecular vibrations within the glass occur.

These give absorption peaks which again extend into the window region. The strong absorption bands occur due to oscillations of structural units such as Si-O (9.2 μm), P-O (8.1 μm), B-O (7.2 μm) and Ge-O (11.0 μm) within the glass. Hence, above 1.5 μm the tails of these largely far-infrared absorption peaks tend to cause most of the pure glass losses. However, the effects of both these processes may be minimized by suitable choice of both core and cladding compositions. For instance, in some non oxide glasses such as fluorides and chlorides, the infrared absorption peaks occur at much longer wavelengths

which are well into the far infrared (up to 50 μm), giving less attenuation to longer wavelength transmission compared with oxide glasses.

2. Extrinsic Absorption

In practical optical fibers prepared by conventional melting techniques, a major source of signal attenuation is extrinsic absorption from transition metal element impurities. Some of the more common metallic impurities found in glasses are shown in the Table 2.1, together with the absorption losses caused by one part.

Table 2.1 Absorption losses caused by some of the more common metallic ion impurities in glasses, together with the absorption peak wavelength

| | <i>Peak wavelength (nm)</i> | <i>One part in 10^9 (dB km^{-1})</i> |
|------------------|-----------------------------|---|
| Cr ³⁺ | 625 | 1.6 |
| C ²⁺ | 685 | 0.1 |
| Cu ²⁺ | 850 | 1.1 |
| Fe ²⁺ | 1100 | 0.68 |
| Fe ³⁺ | 400 | 0.15 |
| Ni ²⁺ | 650 | 0.1 |
| Mn ³⁺ | 460 | 0.2 |
| V ⁴⁺ | 725 | 2.7 |

[Source: <http://img.brainkart.com>]

It may be noted that certain of these impurities, namely chromium and copper, in their worst valence state can cause attenuation in excess of 1 dB km^{-1} in the near-infrared region. Transition element contamination may be reduced to acceptable levels (i.e. one part in 1010) by glass refining techniques such as vapor-phase oxidation, which largely eliminates the effects of these metallic impurities.

However, another major extrinsic loss mechanism is caused by absorption due to water (as the hydroxyl or OH ion) dissolved in the glass. These hydroxyl groups are bonded into the glass structure and have fundamental stretching vibrations which occur at wavelengths between 2.7 and 4.2 μm depending on group position in the glass network. The fundamental vibrations give rise to overtones appearing almost harmonically at 1.38, 0.95 and 0.72 μm , as

illustrated in Figure 2.2. This shows the absorption spectrum for the hydroxyl group in silica.

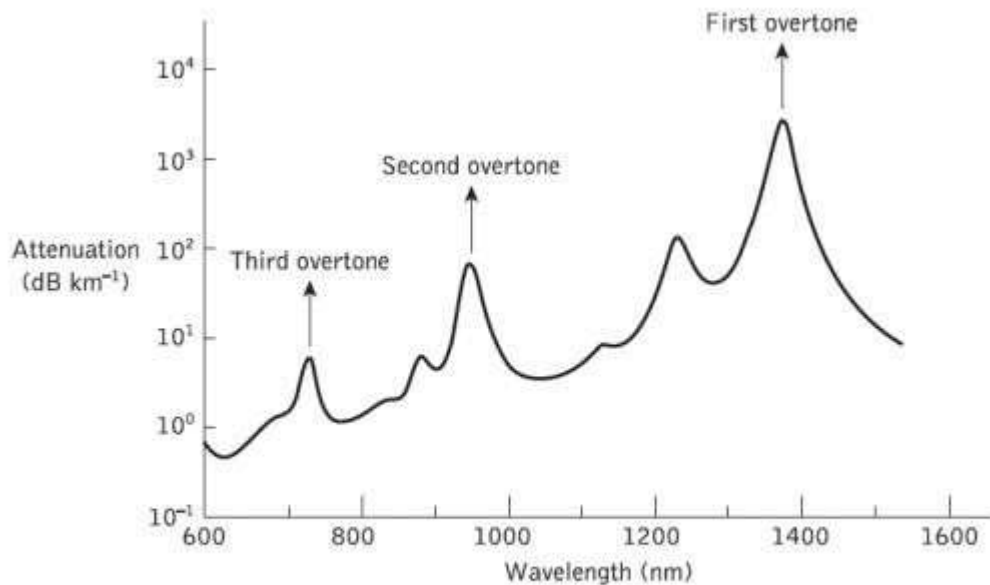


Figure 2.2 The absorption spectrum for the hydroxyl (OH) group in silica.

[Source: <http://img.brainkart.com>]

Furthermore, combinations between the overtones and the fundamental SiO₂ vibration occur at 1.24, 1.13 and 0.88 μm , completing the absorption spectrum shown in Figure 2.2. It may also be observed in Figure 3.2 that the only significant absorption band in the region below a wavelength of 1 μm is the second overtone at 0.95 μm which causes attenuation of about 1 dB km^{-1} for one part per million (ppm) of hydroxyl.

At longer wavelengths the first overtone at 1.383 μm and its sideband at 1.24 μm are strong absorbers giving attenuation of about 2 dB km^{-1} ppm and 4 dB km^{-1} ppm respectively. Since most resonances are sharply peaked, narrow windows exist in the longer wavelength region around 1.31 and 1.55 μm which are essentially unaffected by OH absorption once the impurity level has been reduced below one part in 10⁷.

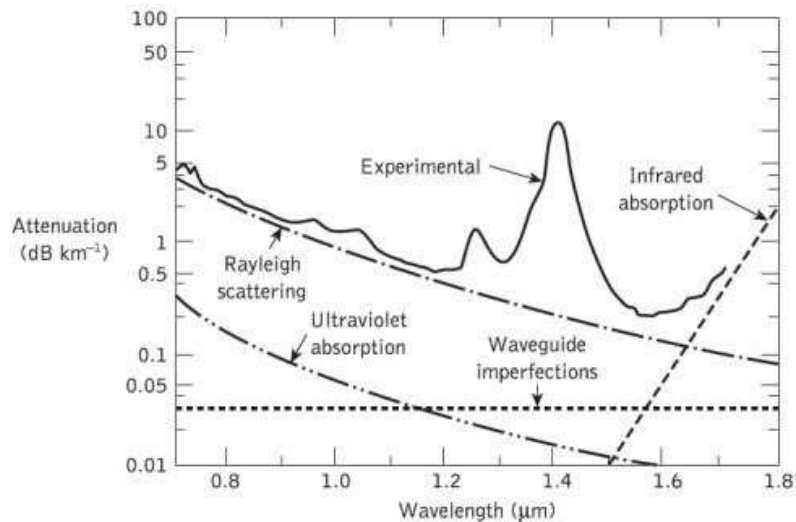


Figure 2.3 The measured attenuation spectrum for an ultra-low-loss single-mode fiber (solid line) with the calculated attenuation spectra for some of the loss mechanisms contributing to the overall fiber attenuation

[Source: <http://img.brainkart.com>]

This situation is illustrated in Figure 2.3, which shows the attenuation spectrum of a low-loss single-mode fiber produced in 1979. It may be observed that the lowest attenuation for this fiber occurs at a wavelength of 1.55 μm and is 0.2 dB km^{-1} . Despite this value approaching the minimum possible attenuation of around 0.18 dB km^{-1} at the 1.55 μm wavelength, it should be noted that the transmission loss of an ultra-low-loss pure silica core fiber was more recently measured as 0.1484 dB km^{-1} at the slightly longer wavelength of 1.57 μm . Although in standard, modern single-mode fibers the loss caused by the primary OH peak at 1.383 μm has been reduced below 1 dB km^{-1} , it still limits operation over significant distances to the lower loss windows at 1.31 and 1.55 μm .

Linear Scattering Losses

Linear scattering mechanisms cause the transfer of some or all of the optical power contained within one propagating mode to be transferred linearly (proportionally to the mode power) into a different mode. This process tends to result in attenuation of the transmitted light as the transfer may be to a leaky or

radiation mode which does not continue to propagate within the fiber core, but is radiated from the fiber. It must be noted that as with all linear processes, there is no change of frequency on scattering. Linear scattering may be categorized into two major types: Rayleigh and Mie scattering. Both result from the nonideal physical properties of the manufactured fiber which are difficult and, in certain cases, impossible to eradicate at present.

1. Rayleigh Scattering

Rayleigh scattering is the dominant intrinsic loss mechanism in the low-absorption window between the ultraviolet and infrared absorption tails. It results from inhomogeneities of a random nature occurring on a small scale compared with the wavelength of the light.

These inhomogeneities manifest themselves as refractive index fluctuations and arise from density and compositional variations which are frozen into the glass lattice on cooling. The compositional variations may be reduced by improved fabrication, but the index fluctuations caused by the freezing-in of density inhomogeneities are fundamental and cannot be avoided.

The subsequent scattering due to the density fluctuations, which is in almost all directions, produces an attenuation proportional to $1/\lambda^4$ following the Rayleigh scattering formula. For a single-component glass this is given by:

$$\gamma_R = \frac{8\pi^3}{3\lambda^4} n^8 p^2 \beta_c K T_F \quad (2.4)$$

where γ_R is the Rayleigh scattering coefficient, λ is the optical wavelength, n is the refractive index of the medium, p is the average photoelastic coefficient, β_c is the isothermal compressibility at a fictive temperature T_F , and K is Boltzmann's constant. The fictive temperature is defined as the temperature at which the glass can reach a state of thermal equilibrium and is closely related to the anneal temperature. Furthermore, the Rayleigh scattering coefficient is

related to the transmission loss factor (transmissivity) of the fiber following the relation:

$$\mathcal{L} = \exp(-\gamma_R L) \quad (2.5)$$

where L is the length of the fiber. It is apparent from Eq. (2.4) that the fundamental component of Rayleigh scattering is strongly reduced by operating at the longest possible wavelength.

2. Mie Scattering

Linear scattering may also occur at inhomogeneities which are comparable in size with the guided wavelength. These result from the nonperfect cylindrical structure of the waveguide and may be caused by fiber imperfections such as irregularities in the core-cladding interface, core-cladding refractive index differences along the fiber length, diameter fluctuations, strains and bubbles. When the scattering inhomogeneity size is greater than $\lambda/10$, the scattered intensity which has an angular dependence can be very large. The scattering created by such inhomogeneities is mainly in the forward direction and is called Mie scattering. Depending upon the fiber material, design and manufacture, Mie scattering can cause significant losses. The inhomogeneities may be reduced by:

- ✓ removing imperfections due to the glass manufacturing process;
- ✓ carefully controlled extrusion and coating of the fiber;
- ✓ increasing the fiber guidance by increasing the relative refractive index difference.

By these means it is possible to reduce Mie scattering to insignificant levels

Nonlinear Scattering Losses

Optical waveguides do not always behave as completely linear channels whose increase in output optical power is directly proportional to the input optical power. Several nonlinear effects occur, which in the case of scattering cause disproportionate attenuation, usually at high optical power levels.

This nonlinear scattering causes the optical power from one mode to be transferred in either the forward or backward direction to the same, or other modes, at a different frequency. It depends critically upon the optical power density within the fiber and hence only becomes significant above threshold power levels.

The most important types of nonlinear scattering within optical fibers are stimulated Brillouin and Raman scattering, both of which are usually only observed at high optical power densities in long single-mode fibers. These scattering mechanisms in fact give optical gain but with a shift in frequency, thus contributing to attenuation for light transmission at a specific wavelength. However, it may be noted that such nonlinear phenomena can also be used to give optical amplification in the context of integrated optical techniques

1. Stimulated Brillouin Scattering

Stimulated Brillouin scattering (SBS) may be regarded as the modulation of light through thermal molecular vibrations within the fiber. The scattered light appears as upper and lower sidebands which are separated from the incident light by the modulation frequency. The incident photon in this scattering process produces a phonon* of acoustic frequency as well as a scattered photon. This produces an optical frequency shift which varies with the scattering angle because the frequency of the sound wave varies with acoustic wavelength.

The frequency shift is a maximum in the backward direction, reducing to zero in the forward direction, making SBS a mainly backward process. As indicated

previously, Brillouin scattering is only significant above a threshold power density. Assuming that the polarization state of the transmitted light is not maintained, it may be shown that the threshold power P_B is given by:

$$P_B = 4.4 \times 10^{-3} d^2 \lambda^2 \alpha_{dB} \nu \text{ watts} \quad (2.6)$$

where d and λ are the fiber core diameter and the operating wavelength, respectively, both measured in micrometers, α_{dB} is the fiber attenuation in decibels per kilometer and ν is the source bandwidth (i.e. injection laser) in gigahertz. The expression given in Eq. (2.6) allows the determination of the threshold optical power which must be launched into a single-mode optical fiber before SBS occurs.

2. Stimulated Raman Scattering

Stimulated Raman scattering (SRS) is similar to SBS except that a high-frequency optical phonon rather than an acoustic phonon is generated in the scattering process. Also, SRS can occur in both the forward and backward directions in an optical fiber, and may have an optical power threshold of up to three orders of magnitude higher than the Brillouin threshold in a particular fiber. Using the same criteria as those specified for the Brillouin scattering threshold given in Eq. (2.6), it may be shown that the threshold optical power for SRS P_R in a long single-mode fiber is given by:

$$P_R = 5.9 \times 10^{-2} d^2 \lambda \alpha_{dB} \text{ watts} \quad (2.7)$$

Fiber Bend Loss

Optical fibers suffer radiation losses at bends or curves on their paths. This is due to the energy in the evanescent field at the bend exceeding the velocity of light in the cladding and hence the guidance mechanism is inhibited, which causes light energy to be radiated from the fiber. An illustration of this situation is shown in Figure 2.5. The part of the mode which is on the outside of the bend is required to travel faster than that on the inside so that a wavefront perpendicular to the direction of propagation is maintained.

Hence, part of the mode in the cladding needs to travel faster than the velocity of light in that medium. As this is not possible, the energy associated with this part of the mode is lost through radiation. The loss can generally be represented by a radiation attenuation coefficient which has the form:

$$\alpha_r = c_1 \exp(-c_2 R)$$

Where R is the radius of curvature of the fiber bend and c_1 , c_2 are constants which are independent of R . Furthermore, large bending losses tend to occur in multimode fibers at a critical radius of curvature R_c which may be estimated from:

$$R_c \approx \frac{3n_1^2 \lambda}{4\pi(n_1^2 - n_2^2)^{3/2}} \quad (2.8)$$

It may be observed from the expression given in Eq. (2.8) that potential macrobending losses may be reduced by:

- ✓ designing fibers with large relative refractive index differences;
- ✓ operating at the shortest wavelength possible.

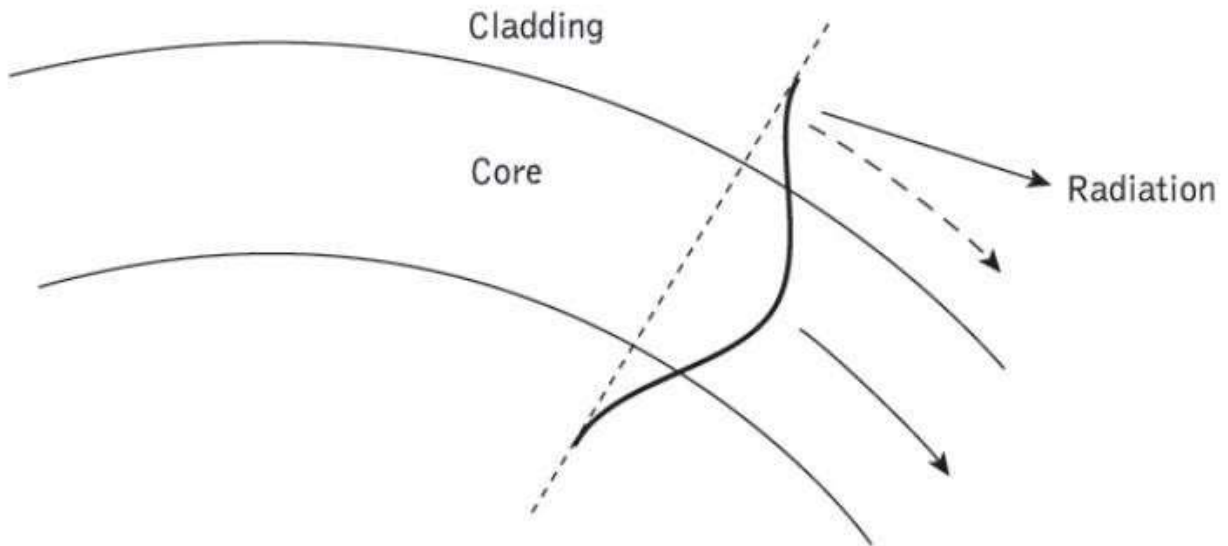


Figure 2.5 An illustration of the radiation loss at a fiber bend.

[Source: <http://img.brainkart.com>]

The above criteria for the reduction of bend losses also apply to single-mode fibers. One theory, based on the concept of a single quasi-guided mode, provides an expression from which the critical radius of curvature for a single-mode fiber R_{cs} can be estimated as

$$R_{cs} = \frac{20\lambda}{(n_1 - n_2)^3} \left(2.748 - 0.996 \frac{\lambda}{\lambda_c} \right)^{-3} \quad (2.9)$$

where λ_c is the cutoff wavelength for the single-mode fiber. Hence again, for a specific single-mode fiber (i.e. a fixed relative index difference and cutoff wavelength), the critical wavelength of the radiated light becomes progressively shorter as the bend radius is decreased.

Mid-Infrared and Far-Infrared Transmission

In the near-infrared region of the optical spectrum, fundamental silica fiber attenuation is dominated by Rayleigh scattering and multiphonon absorption from the infrared absorption edge (see Figure 2.2). Therefore, the total loss decreases as the operational transmission wavelength increases until a crossover point is reached around a wavelength of 1.55 μm where the total fiber loss again increases because at longer wavelengths the loss is dominated by the phonon absorption edge. Since the near fundamental attenuation limits for near-infrared silicate class fibers have been achieved, more recently researchers have turned their attention to the mid-infrared (2 to 5 μm) and the far-infrared (8 to 12 μm) optical wavelengths.

In order to obtain lower loss fibers it is necessary to produce glasses exhibiting longer infrared cutoff wavelengths. Potentially, much lower losses can be achieved if the transmission window of the material can be extended further into the infrared by utilizing constituent atoms of higher atomic mass and if it can be drawn into fiber exhibiting suitable strength and chemical durability. The reason for this possible loss reduction is due to Rayleigh scattering which displays a λ^{-4} dependence and hence becomes much reduced as the wavelength is increased. For example, the scattering loss is reduced by a factor of 16 when the optical wavelength is doubled.

Thus it may be possible to obtain losses of the order of 0.01 dB km^{-1} at a wavelength of 2.55 μm , with even lower losses at wavelengths of between 3 and 5 μm . Candidate glass-forming systems for mid-infrared transmission are fluoride, fluoride–chloride, chalcogenide and oxide.

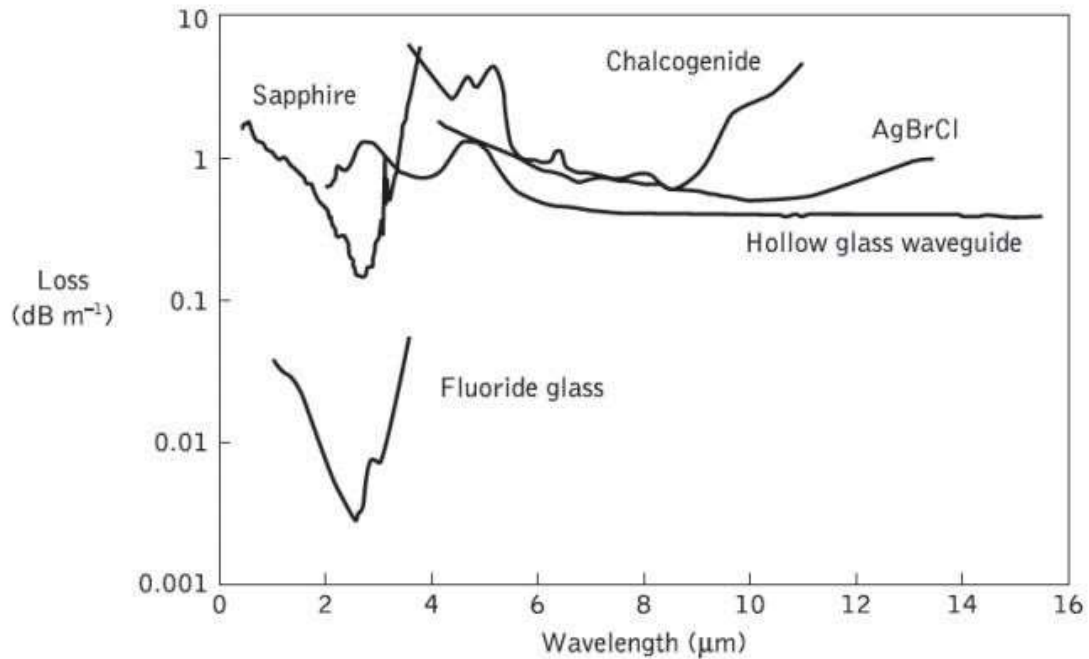


Figure 2.6 Attenuation spectra for some common mid- and far-infrared fibers

[Source: <http://img.brainkart.com>]

In particular, oxide glasses such as Al_2O_3 (i.e. sapphire) offer a near equivalent transmittance range to many of the fluoride glasses and have benefits of high melting points, chemical inertness, and the ability to be readily melted and grown in air. Chalcogenide glasses, which generally comprise one or more elements Ge, Si, As and Sb, are capable of optical transmission in both the mid-infrared and far-infrared regions.

A typical chalcogenide fiber glass is therefore arsenide trisulfide (As_2S_3). However, research activities into far-infrared transmission using chalcogenide glasses, halide glasses, polycrystalline halide fibers (e.g. silver and thallium) and hollow glass waveguides are primarily concerned with radiometry, infrared imaging, optical wireless, optical sensing and optical power transmission rather than telecommunications

The loss spectrum for a single-crystal sapphire fiber which also transmits in the midinfrared is also shown in Figure 2.6. Although they have robust physical properties, including a Young's modulus six times greater as well as a thermal expansion some ten times higher than that of silica, these fibers lend themselves

to optical power delivery applications [Ref. 27], not specifically optical communications. Chalcogenide glasses which have their lowest losses over both the mid- and far-infrared ranges are very stable, durable and insensitive to moisture. Arsenic trisulfide fiber, being one of the simplest, has a spectral range from 0.7 to around 6 μm . Hence it has a cut off at long wavelength significantly before the chalcogenide fibers containing heavier elements such as Te, Ge and Se, an attenuation spectrum for the latter being incorporated in Figure 2.6. In general, chalcogenide glass fibers have proved to be useful in areas such as optical sensing, infrared imaging and for the production of fiber infrared lasers and amplifiers.

www.binils.com

Dispersion

Dispersion of the transmitted optical signal causes distortion for both digital and analog transmission along optical fibers. When considering the major implementation of optical fiber transmission which involves some form of digital modulation, then dispersion mechanisms within the fiber cause broadening of the transmitted light pulses as they travel along the channel. The phenomenon is illustrated in Figure 2.7, where it may be observed that each pulse broadens and overlaps with its neighbors, eventually becoming indistinguishable at the receiver input. The effect is known as intersymbol interference (ISI). Thus an increasing number of errors may be encountered on the digital optical channel as the ISI becomes more pronounced. The error rate is also a function of the signal attenuation on the link and the subsequent signal-to-noise ratio (SNR) at the receiver. For no overlapping of light pulses down an optical fiber link the digital bit rate BT must be less than the reciprocal of the broadened (through dispersion) pulse duration (2τ).

Hence:

$$B_T \leq \frac{1}{2\tau} \quad (2.10)$$

The conversion of bit rate to bandwidth in hertz depends on the digital coding format used. For metallic conductors when a nonreturn-to-zero code is employed, the binary 1 level is held for the whole bit period τ . In this case there are two bit periods in one wavelength (i.e. 2 bits per second per hertz), as illustrated in Figure 2.8(a). Hence the maximum bandwidth B is one-half the maximum data rate or:

$$B_T(\text{max}) = 2B \tag{2.12}$$

However, when a return-to-zero code is considered, as shown in Figure 2.8(b), the binary 1 level is held for only part (usually half) of the bit period. For this signaling scheme the data rate is equal to the bandwidth in hertz (i.e. 1 bit per second per hertz) and thus $BT = B$.

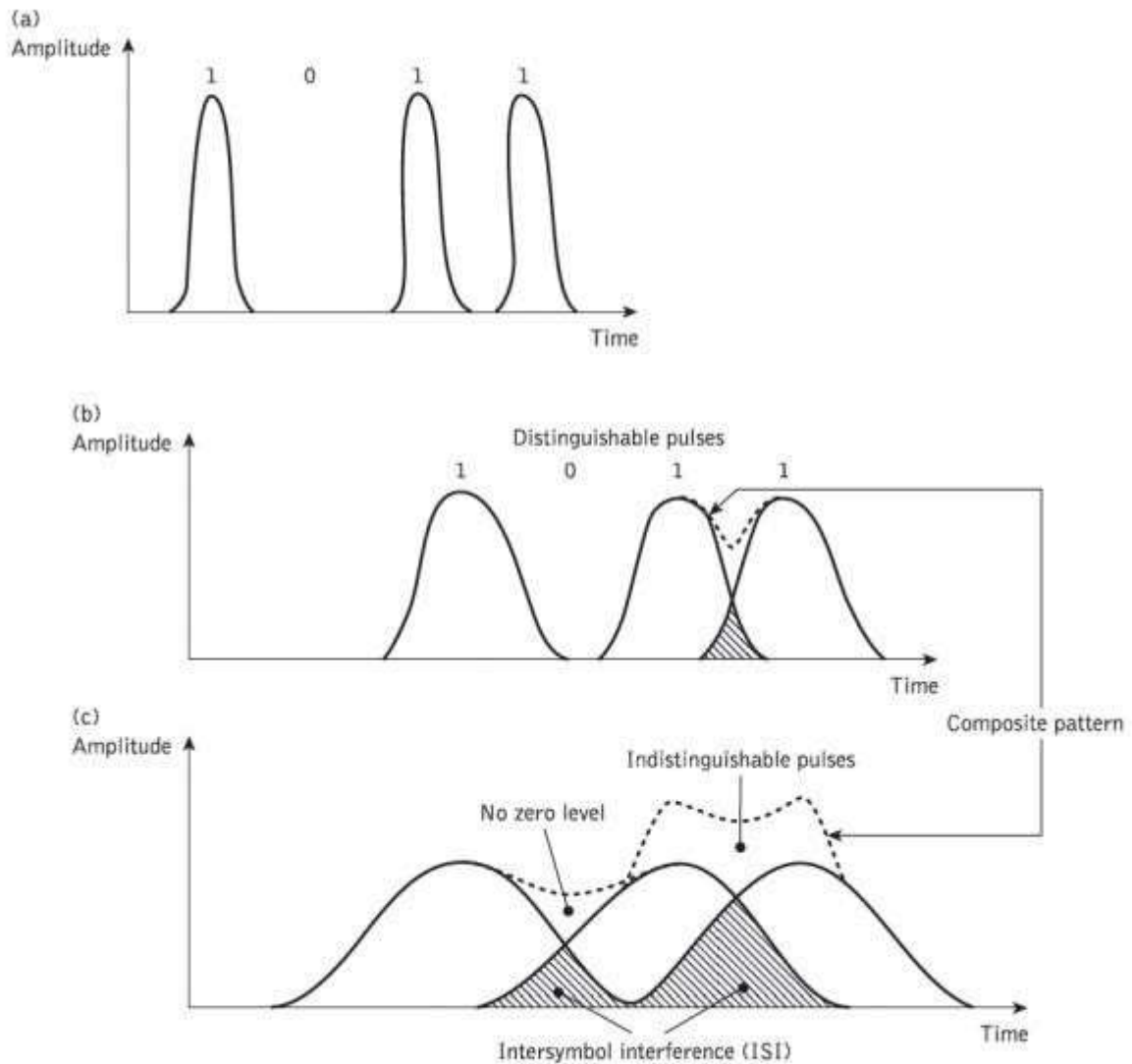


Figure 2.7 An illustration using the digital bit pattern 1011 of the broadening of light pulses as they are transmitted along a fiber: (a) fiber input; (b) fiber output at a distance L_1 ; (c) fiber output at a distance $L_2 > L_1$

[Source: <http://img.brainkart.com>]

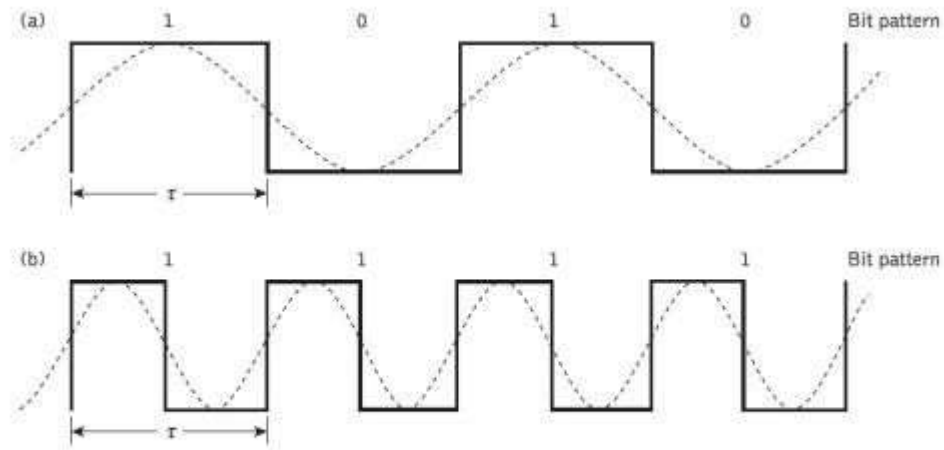


Figure 2.8 Schematic illustration of the relationships of the bit rate to wavelength for digital codes: (a) nonreturn-to-zero (NRZ), (b) return-to-zero (RZ)

[Source: <http://img.brainkart.com>]

The bandwidth B for metallic conductors is also usually defined by the electrical 3 Db points (i.e. the frequencies at which the electric power has dropped to one-half of its constant maximum value). However, when the 3 dB optical bandwidth of a fiber is considered it is significantly larger than the corresponding 3 dB electrical bandwidth. Hence, when the limitations in the bandwidth of a fiber due to dispersion are stated (i.e. optical bandwidth B_{opt}), it is usually with regard to a return to zero code where the bandwidth in hertz is considered equal to the digital bit rate. Within the context of dispersion the bandwidths expressed in this chapter will follow this general criterion unless otherwise stated. when electro-optic devices and optical fiber systems are considered it is more usual to state the electrical 3 dB bandwidth, this being the more useful measurement when interfacing an optical fiber link to electrical terminal equipment.

Intramodal Dispersion

Chromatic or intramodal dispersion may occur in all types of optical fiber and results from the finite spectral linewidth of the optical source. Since optical sources do not emit just a single frequency but a band of frequencies (in the case of the injection laser corresponding to only a fraction of a percent of the center frequency, whereas for the LED it is likely to be a significant percentage), then there may be propagation delay differences between the different spectral components of the transmitted signal. This causes broadening of each transmitted mode and hence intramodal dispersion. The delay differences may be caused by the dispersive properties of the waveguide material (material dispersion) and also guidance effects within the fiber structure (waveguide dispersion).

1. Material Dispersion

Pulse broadening due to material dispersion results from the different group velocities of the various spectral components launched into the fiber from the optical source. It occurs when the phase velocity of a plane wave propagating in the dielectric medium varies nonlinearly with wavelength, and a material is said to exhibit material dispersion when the second differential of the refractive index with respect to wavelength is not zero.

Hence the group delay is given by:

$$\tau_g = \frac{d\beta}{d\omega} = \frac{1}{c} \left(n_1 - \lambda \frac{dn_1}{d\lambda} \right) \quad (2.13)$$

Where n_1 is the refractive index of the core material. The pulse delay τ_m due to material dispersion in a fiber of length L is therefore:

$$\tau_m = \frac{L}{c} \left(n_1 - \lambda \frac{dn_1}{d\lambda} \right) \quad (2.14)$$

For a source with rms spectral width σ_λ and a mean wavelength λ , the rms pulse broadening due to material dispersion σ_m may be obtained from the expansion of Eq. (2.14) in a Taylor series about where:

$$\sigma_m = \sigma_\lambda \frac{d\tau_m}{d\lambda} + \sigma_\lambda \frac{2d^2\tau_m}{d\lambda^2} + \dots \quad (2.15)$$

As the first term in Eq. (2.15) usually dominates, especially for sources operating over the 0.8 to 0.9 μm wavelength range, then:

$$\sigma_m \approx \sigma_\lambda \frac{d\tau_m}{d\lambda} \quad (2.16)$$

Hence the pulse spread may be evaluated by considering the dependence of τ_m on λ , where from Eq. (2.14):

$$\begin{aligned} \frac{d\tau_m}{d\lambda} &= \frac{L\lambda}{c} \left[\frac{dn_1}{d\lambda} - \frac{d^2n_1}{d\lambda^2} - \frac{dn_1}{d\lambda} \right] \\ &= \frac{-L\lambda}{c} \frac{d^2n_1}{d\lambda^2} \end{aligned} \quad (2.17)$$

Therefore, substituting the expression obtained in Eq. (2.17) into Eq. (2.16), the rms pulse broadening due to material dispersion is given by:

$$\sigma_m \cong \frac{\sigma_\lambda L}{c} \left| \lambda \frac{d^2 n_1}{d\lambda^2} \right| \quad (2.18)$$

The material dispersion for optical fibers is sometimes quoted as a value for $|\lambda^2(d^2 n_1/d\lambda^2)|$ or simply $|d^2 n_1/d\lambda^2|$.

However, it may be given in terms of a material dispersion parameter M which is defined as:

$$M = \frac{1}{L} \frac{d\tau_m}{d\lambda} = \frac{\lambda}{c} \left| \frac{d^2 n_1}{d\lambda^2} \right| \quad (2.19)$$

and which is often expressed in units of ps nm⁻¹ km⁻¹.

2. Waveguide Dispersion

The wave guiding of the fiber may also create chromatic dispersion. This results from the variation in group velocity with wavelength for a particular mode. Considering the ray theory approach, it is equivalent to the angle between the ray and the fiber axis varying with wavelength which subsequently leads to a variation in the transmission times for the rays, and hence dispersion. For a single mode whose propagation constant is β , the fiber exhibits waveguide dispersion when $d^2\beta/d\lambda^2 \neq 0$. Multimode fibers, where the majority of modes propagate far from cutoff, are almost free of waveguide dispersion and it is generally negligible compared with material dispersion (≈ 0.1 to 0.2 ns/km). However, with single-mode fibers where the effects of the different dispersion mechanisms are not easy to separate, waveguide dispersion may be significant.

Intermodal Dispersion

Pulse broadening due to intermodal dispersion (sometimes referred to simply as modal or mode dispersion) results from the propagation delay differences between modes within a multimode fiber. As the different modes which constitute a pulse in a multimode fiber travel along the channel at different group velocities, the pulse width at the output is dependent upon the transmission times of the slowest and fastest modes. This dispersion mechanism creates the fundamental difference in the overall dispersion for the three types

of fiber. Thus multimode step index fibers exhibit a large amount of intermodal dispersion which gives the greatest pulse broadening. However, intermodal dispersion in multimode fibers may be reduced by adoption of an optimum refractive index profile which is provided by the near-parabolic profile of most graded index fibers.

Hence, the overall pulse broadening in multimode graded index fibers is far less than that obtained in multimode step index fibers (typically by a factor of 100). Thus graded index fibers used with a multimode source give a tremendous bandwidth advantage over multimode step index fibers. Under purely single-mode operation there is no intermodal dispersion and therefore pulse broadening is solely due to the intramodal dispersion mechanisms. In theory, this is the case with single-mode step index fibers where only a single mode is allowed to propagate. Hence they exhibit the least pulse broadening and have the greatest possible bandwidths, but in general are only usefully operated with single-mode sources. In order to obtain a simple comparison for intermodal pulse broadening between multimode step index and multimode graded index fibers, it is useful to consider the geometric optics picture for the two types of fiber.

1. Multimode Step Index Fiber

Using the ray theory model, the fastest and slowest modes propagating in the step index fiber may be represented by the axial ray and the extreme meridional ray (which is incident at the core-cladding interface at the critical angle ϕ_c) respectively. The paths taken by these two rays in a perfectly structured step index fiber are shown in Figure 2.9. The delay difference between these two rays when traveling in the fiber core allows estimation of the pulse broadening resulting from intermodal dispersion within the fiber. As both rays are traveling at the same velocity within the constant refractive index fiber core, then the

delay difference is directly related to their respective path lengths within the fiber. Hence the time taken for the axial ray to travel along a fiber of length L gives the minimum delay time T_{Min} and:

$$T_{\text{Min}} = \frac{\text{distance}}{\text{velocity}} = \frac{L}{(c/n_1)} = \frac{Ln_1}{c} \quad (2.20)$$

where n_1 is the refractive index of the core and c is the velocity of light in a vacuum. The extreme meridional ray exhibits the maximum delay time T_{Max} where:

$$T_{\text{Max}} = \frac{L/\cos \theta}{c/n_1} = \frac{Ln_1}{c \cos \theta} \quad (2.21)$$

Using Snell's law of refraction at the core-cladding interface following Eq. (2.2):

$$\sin \phi_c = \frac{n_2}{n_1} = \cos \theta \quad (2.22)$$

where n_2 is the refractive index of the cladding. Furthermore, substituting into Eq. (2.21) gives:

$$T_{\text{Max}} = \frac{Ln_1^2}{cn_2} \quad (2.23)$$

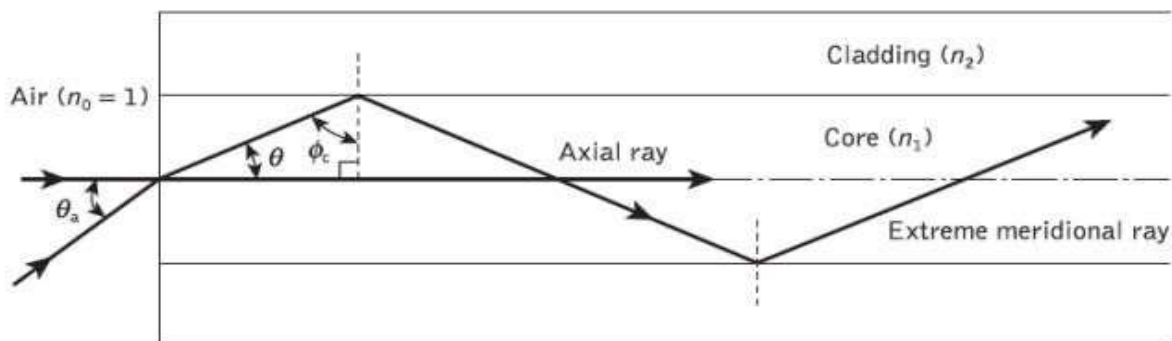


Figure 2.9 The paths taken by the axial and an extreme meridional ray in a perfect multimode step index fiber

[Source: <http://img.brainkart.com>]

The delay difference T_s between the extreme meridional ray and the axial ray may be obtained by:

$$\begin{aligned} \delta T_s = T_{\text{Max}} - T_{\text{Min}} &= \frac{Ln_1^2}{cn_2} - \frac{Ln_1}{c} \\ &= \frac{Ln_1^2}{cn_2} \left(\frac{n_1 - n_2}{n_1} \right) \end{aligned} \quad (2.24)$$

$$\approx \frac{Ln_1^2 \Delta}{cn_2} \quad \text{when } \Delta \ll 1 \quad (2.25)$$

where Δ is the relative refractive index difference. However, when $\Delta \ll 1$, then from the definition given by Eq. (2.9), the relative refractive index difference may also be given approximately by:

$$\Delta \approx \frac{n_1 - n_2}{n_2} \quad (2.26)$$

Hence rearranging Eq. (2.24):

$$\delta T_s = \frac{Ln_1}{c} \left(\frac{n_1 - n_2}{n_2} \right) \approx \frac{Ln_1 \Delta}{c} \quad (2.27)$$

Also substituting for Δ from Eq. (2.10) gives:

$$\delta T_s \approx \frac{L(NA)^2}{2n_1 c} \quad (2.28)$$

where NA is the numerical aperture for the fiber. The approximate expressions for the delay difference given in Eqs (2.27) and (2.28) are usually employed to estimate the maximum pulse broadening in time due to intermodal dispersion in multimode step index fibers. Again considering the perfect step index fiber, another useful quantity with regard to intermodal dispersion on an optical fiber link is the rms pulse broadening resulting from this dispersion mechanism along the fiber. When the optical input to the fiber is a pulse $p_i(t)$ of unit area, as illustrated in Figure 2.10, then

$$\int_{-\infty}^{\infty} p_1(t) dt = 1 \quad (2.29)$$

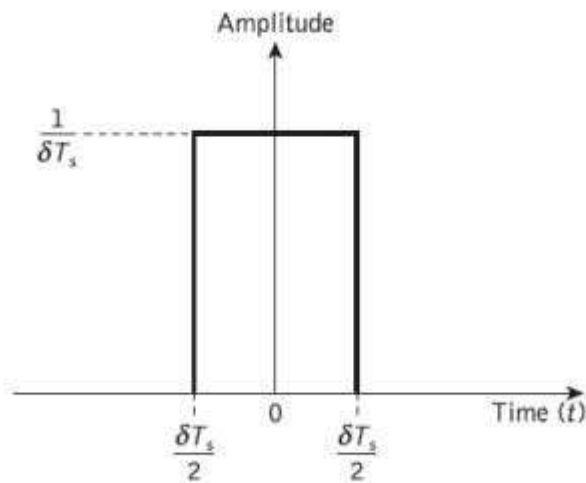


Figure 2.10 An illustration of the light input to the multimode step index fiber consisting of an ideal pulse or rectangular function with unit area

[Source: <http://img.brainkart.com>]

It may be noted that $p_1(t)$ has a constant amplitude of $1/T_s$ over the range:

$$-\frac{\delta T_s}{2} \leq p(t) \leq \frac{\delta T_s}{2}$$

The rms pulse broadening at the fiber output due to intermodal dispersion for the multimode step index fiber (i.e. the standard deviation) may be given in terms of the variance σ_s^2 :

$$\sigma_s^2 = M_2 - M_1^2 \quad (2.30)$$

Where M_1 is the first temporal moment which is equivalent to the mean value of the pulse and M_2 , the second temporal moment, is equivalent to the mean square value of the pulse.

Hence:

$$M_1 = \int_{-\infty}^{\infty} t p_1(t) dt \quad (2.31)$$

And:

$$M_2 = \int_{-\infty}^{\infty} t^2 p_1(t) dt \quad (2.32)$$

The mean value M_1 for the unit input pulse of Figure 2.10 is zero, and assuming this is maintained for the output pulse, then from Eqs (2.30) and (2.32):

$$\sigma_s^2 = M_2 = \int_{-\infty}^{\infty} t^2 p_1(t) dt \quad (2.33)$$

Integrating over the limits of the input pulse (Figure 3.12) and substituting for $p_1(t)$ in Eq. (2.33) over this range gives:

$$\begin{aligned} \sigma_s^2 &= \int_{-\delta T_s/2}^{\delta T_s/2} \frac{1}{\delta T_s} t^2 dt \\ &= \frac{1}{\delta T_s} \left[\frac{t^3}{3} \right]_{-\delta T_s/2}^{\delta T_s/2} = \frac{1}{3} \left(\frac{\delta T_s}{2} \right)^2 \end{aligned} \quad (2.34)$$

Hence substituting from Eq. (2.27) for δT_s gives:

$$\sigma_s \approx \frac{L n_1 \Delta}{2\sqrt{3}c} \approx \frac{L(NA)^2}{4\sqrt{3}n_1 c} \quad (2.35)$$

Equation (2.35) allows estimation of the rms impulse response of a multimode step index fiber if it is assumed that intermodal dispersion dominates and there is a uniform distribution of light rays over the range. The pulse broadening is directly proportional to the relative refractive index difference and the length of the fiber L . The latter emphasizes the bandwidth–length trade-off that exists, especially with multimode step index fibers, and which inhibits their use for wideband long-haul (between repeaters) systems. Furthermore, the pulse broadening is reduced by reduction of the relative refractive index

difference for the fiber. Intermodal dispersion may be reduced by propagation mechanisms within practical fibers. For instance, there is differential attenuation of the various modes in a step index fiber. This is due to the greater field penetration of the higher order modes into the cladding of the waveguide. These slower modes therefore exhibit larger losses at any core–cladding irregularities, which tends to concentrate the transmitted optical power into the faster lower order modes. Thus the differential attenuation of modes reduces intermodal pulse broadening on a multimode optical link.

Another mechanism which reduces intermodal pulse broadening in nonperfect (i.e. practical) multimode fibers is the mode coupling or mixing. The coupling between guided modes transfers optical power from the slower to the faster modes, and vice versa. Hence, with strong coupling the optical power tends to be transmitted at an average speed, which is the mean of the various propagating modes. This reduces the intermodal dispersion on the link and makes it advantageous to encourage mode coupling within multimode fibers. The expression for delay difference given in Eq. (2.27) for a perfect step index fiber may be modified for the fiber with mode coupling among all guided modes to:

$$\delta T_{sc} \approx \frac{n_1 \Delta}{c} (LL_c)^{\frac{1}{2}} \quad (2.36)$$

2. Multimode Graded Index Fiber

Intermodal dispersion in multimode fibers is minimized with the use of graded index fibers. Hence, multimode graded index fibers show substantial bandwidth improvement over multimode step index fibers. The reason for the improved performance of graded index fibers may be observed by considering the ray diagram for a graded index fiber shown in Figure 2.11. The fiber shown has a parabolic index profile with a maximum at the core axis, as illustrated in Figure 2.11(a). Analytically, the index profile is given by:

$$\begin{aligned}
 n(r) &= n_1[1 - 2\Delta(r/a)^2]^{\frac{1}{2}} & r < a \text{ (core)} \\
 &= n_1(1 - 2\Delta)^{\frac{1}{2}} = n_2 & r \geq a \text{ (cladding)}
 \end{aligned}
 \tag{2.37}$$

Figure 2.11(b) shows several meridional ray paths within the fiber core. It may be observed that apart from the axial ray, the meridional rays follow sinusoidal trajectories of different path lengths which result from the index grading. However, the local group velocity is inversely proportional to the local refractive index and therefore the longer sinusoidal paths are compensated for by higher speeds in the lower index medium away from the axis.

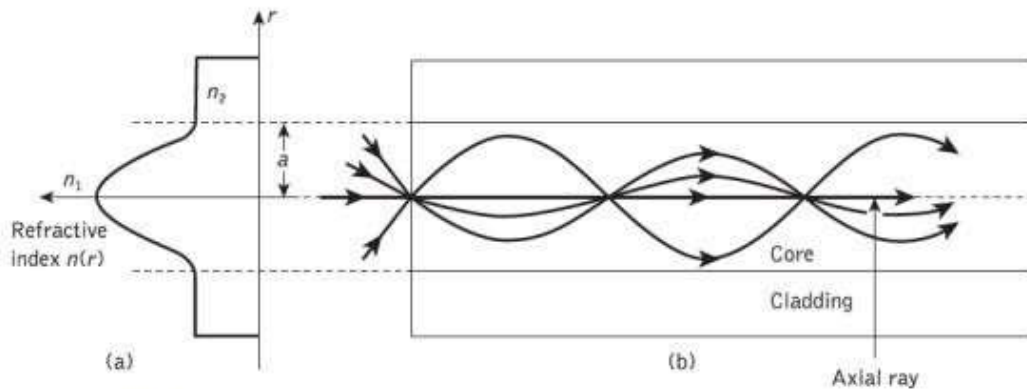


Figure 2.11 A multimode graded index fiber: (a) parabolic refractive index profile; (b) meridional ray paths within the fiber core

[Source: <http://img.brainkart.com>]

Hence there is an equalization of the transmission times of the various trajectories towards the transmission time of the axial ray which travels exclusively in the high-index region at the core axis, and at the slowest speed. As these various ray paths may be considered to represent the different modes propagating in the fiber, then the graded profile reduces the disparity in the mode transit times. The dramatic improvement in multimode fiber bandwidth achieved with a parabolic or near-parabolic refractive index profile is highlighted by consideration of the reduced delay difference between the fastest and slowest modes for this graded index fiber T_g . Using a ray theory approach the delay difference is given by:

$$\delta T_g \approx \frac{Ln_1\Delta^2}{2c} \approx \frac{(NA)^4}{8n_1^3c} \quad (2.38)$$

However, a more rigorous analysis using electromagnetic mode theory gives an absolute temporal width at the fiber output of :

$$\delta T_g = \frac{Ln_1\Delta^2}{8c} \quad (2.39)$$

which corresponds to an increase in transmission time for the slowest mode of $2/8$ over the fastest mode. The expression given in Eq. (2.39) does not restrict the bandwidth to pulses with time slots corresponding to T_g as 70% of the optical power is concentrated in the first half of the interval. Hence the rms pulse broadening is a useful parameter for assessment of intermodal dispersion in multimode graded index fibers. It may be shown that the rms pulse broadening of a near-parabolic index profile graded index fiber g is reduced compared with similar broadening for the corresponding step index fibers (i.e. with the same relative refractive index difference) following

$$\sigma_g = \frac{\Delta}{D} \sigma_s \quad (2.40)$$

where D is a constant between 4 and 10 depending on the precise evaluation and the exact optimum profile chosen. The best minimum theoretical intermodal rms pulse broadening for a graded index fiber with an optimum characteristic refractive index profile for the core α_{op} of

$$\alpha_{op} = 2 - \frac{12\Delta}{5} \quad (2.41)$$

is given by combining Eqs (2.27) and (2.40) as:

$$\sigma_g = \frac{Ln_1\Delta^2}{20\sqrt{3}c} \quad (2.42)$$

Fiber Connectors

Demountable fiber connectors are more difficult to achieve than optical fiber splices. This is because they must maintain similar tolerance requirements to splices in order to couple light between fibers efficiently, but they must accomplish it in a removable fashion. Also, the connector design must allow for repeated connection and disconnection without problems of fiber alignment, which may lead to degradation in the performance of the transmission line at the joint. Hence to operate satisfactorily the demountable connector must provide reproducible accurate alignment of the optical fibers.

In order to maintain an optimum performance the connection must also protect the fiber ends from damage which may occur due to handling (connection and disconnection), must be insensitive to environmental factors (e.g. moisture and dust) and must cope with tensile load on the cable. Additionally, the connector should ideally be a low-cost component which can be fitted with relative ease. Hence optical fiber connectors may be considered in three major areas, which are:

- ✓ the fiber termination, which protects and locates the fiber ends;
- ✓ the fiber end alignment to provide optimum optical coupling;
- ✓ the outer shell, which maintains the connection and the fiber alignment, protects the fiber ends from the environment and provides adequate strength at the joint.

1. Cylindrical Ferrule Connectors

The basic ferrule connector (sometimes referred to as a concentric sleeve connector), which is perhaps the simplest optical fiber connector design. The two fibers to be connected are permanently bonded (with epoxy resin) in metal plugs known as ferrules which have an accurately drilled central hole in

their end faces where the stripped (of buffer coating) fiber is located. Within the connector the two ferrules are placed in an alignment sleeve which, using accurately machined components, allows the fiber ends to be butt jointed. The ferrules are held in place via a retaining mechanism which, in the example shown in Figure 2.29(a), is a spring.

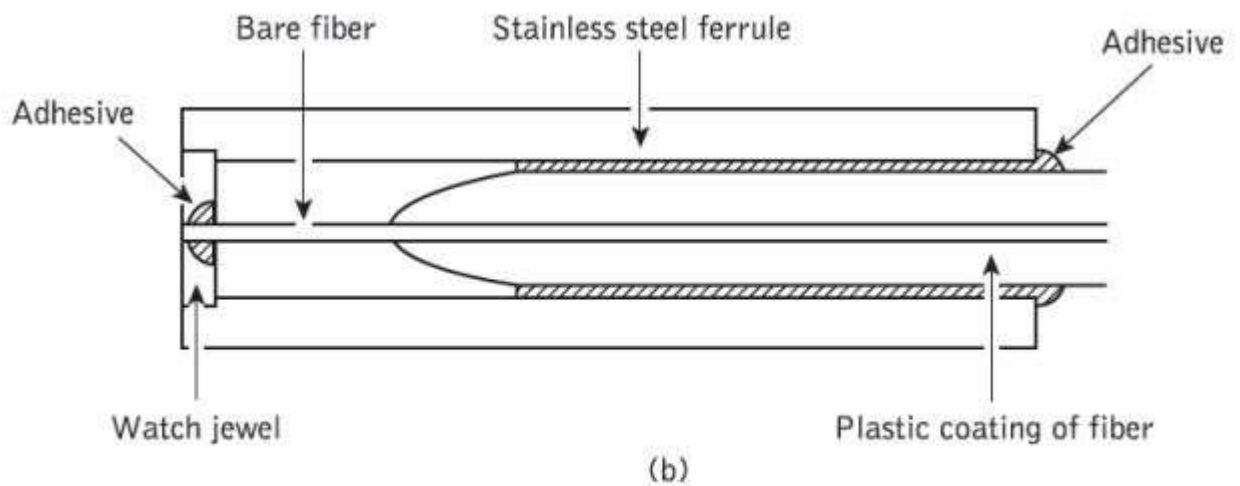
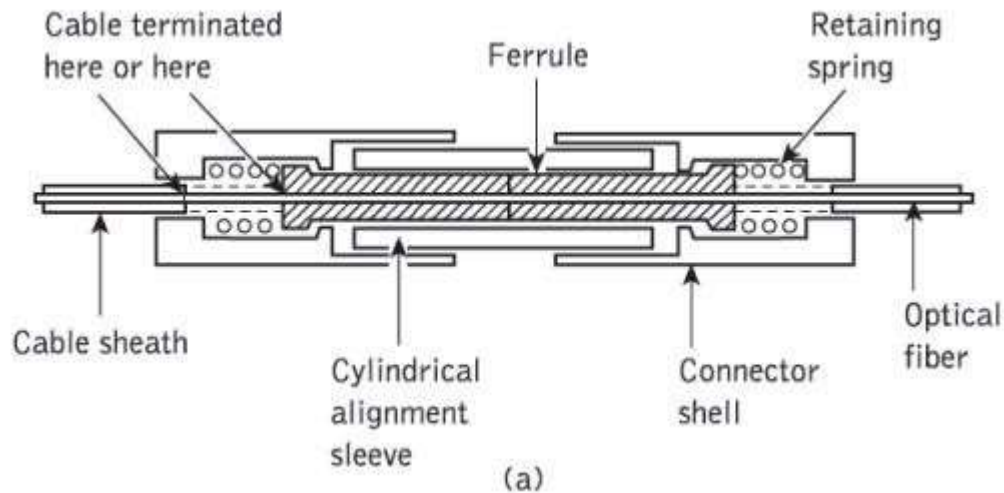


Figure 2.29 Ferrule connectors: (a) structure of a basic ferrule connector; (b) structure of a watch jewel connector ferrule

[Source: <http://img.brainkart.com>]

It is essential with this type of connector that the fiber end faces are smooth and square (i.e. perpendicular to the fiber axis). This may be achieved with varying success by:

- ✓ cleaving the fiber before insertion into the ferrule;
- ✓ inserting and bonding before cleaving the fiber close to the ferrule end face;
- ✓ using either (a) or (b) and polishing the fiber end face until it is flush with the end of the ferrule.

Polishing the fiber end face after insertion and bonding provides the best results but it tends to be time consuming and inconvenient, especially in the field. The fiber alignment accuracy of the basic ferrule connector is largely dependent upon the ferrule hole into which the fiber is inserted. Hence, some ferrule connectors have incorporated a watch jewel in the ferrule end face (jeweled ferrule connector), as illustrated in Figure 2.29(b). In this case the fiber is centered with respect to the ferrule through the watch jewel hole. The use of the watch jewel allows the close diameter and tolerance requirements of the ferrule end face hole to be obtained more easily than simply through drilling of the metallic ferrule end face alone. Nevertheless, typical concentricity errors between the fiber core and the outside diameter of the jeweled ferrule are in the range 2 to 6 μm giving insertion losses in the range 1 to 2 dB with multimode step index fibers

2. Expanded Beam Connectors

An alternative to connection via direct butt joints between optical fibers is offered by the principle of the expanded beam. Fiber connection utilizing this principle is illustrated in Figure 2.30, which shows a connector consisting of two lenses for collimating and refocusing the light from one fiber into the other. The use of these interposed optics makes the achievement of lateral alignment much less critical than with a butt-jointed fiber connector.

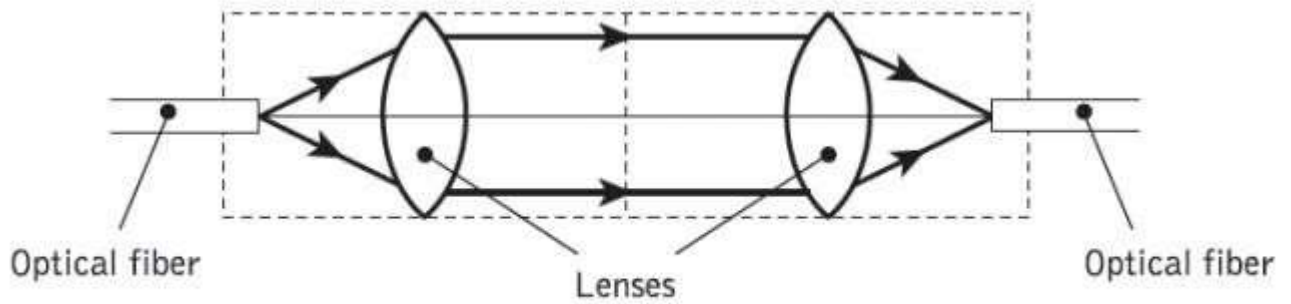


Figure 2.30 Schematic illustration of an expanded beam connector showing the principle of operation

[Source: <http://img.brainkart.com>]

Also, the longitudinal separation between the two mated halves of the connector ceases to be critical. However, this is achieved at the expense of more stringent angular alignment. Nevertheless, expanded beam connectors are useful for multifiber connection and edge connection for printed circuit boards where lateral and longitudinal alignment are frequently difficult to achieve.

Two examples of lens-coupled expanded beam connectors are illustrated in Figure 2.31. The connector shown in Figure 2.31(a) utilized spherical microlenses for beam expansion and reduction. It exhibited average losses of 1 dB which were reduced to 0.7 dB with the application of an antireflection coating on the lenses and the use of graded index fiber of 50 μm core diameter. A similar configuration has been used for single-mode fiber connection in which the lenses have a 2.5 mm diameter. Again with antireflection-coated lenses, average losses around 0.7 dB were obtained using single-mode fibers of 8 μm core diameter. Furthermore, successful single-mode fiber

connection has been achieved with a much smaller (250 μm diameter) sapphire ball lens expanded beam design. In this case losses in the range 0.4 to 0.7 dB were demonstrated over 1000 connections. Figure 2.31(b) shows an expanded beam connector which employs a molded spherical lens. The fiber is

positioned approximately at the focal length of the lens in order to obtain a collimated beam and hence minimize lens-to-lens longitudinal misalignment effects. A lens alignment sleeve is used to minimize the effects of angular misalignment which, together with a ferrule, grommet, spring and external housing, provides the complete connector structure. The repeatability of this relatively straightforward lens design was found to be good, incurring losses of around 0.7 dB.

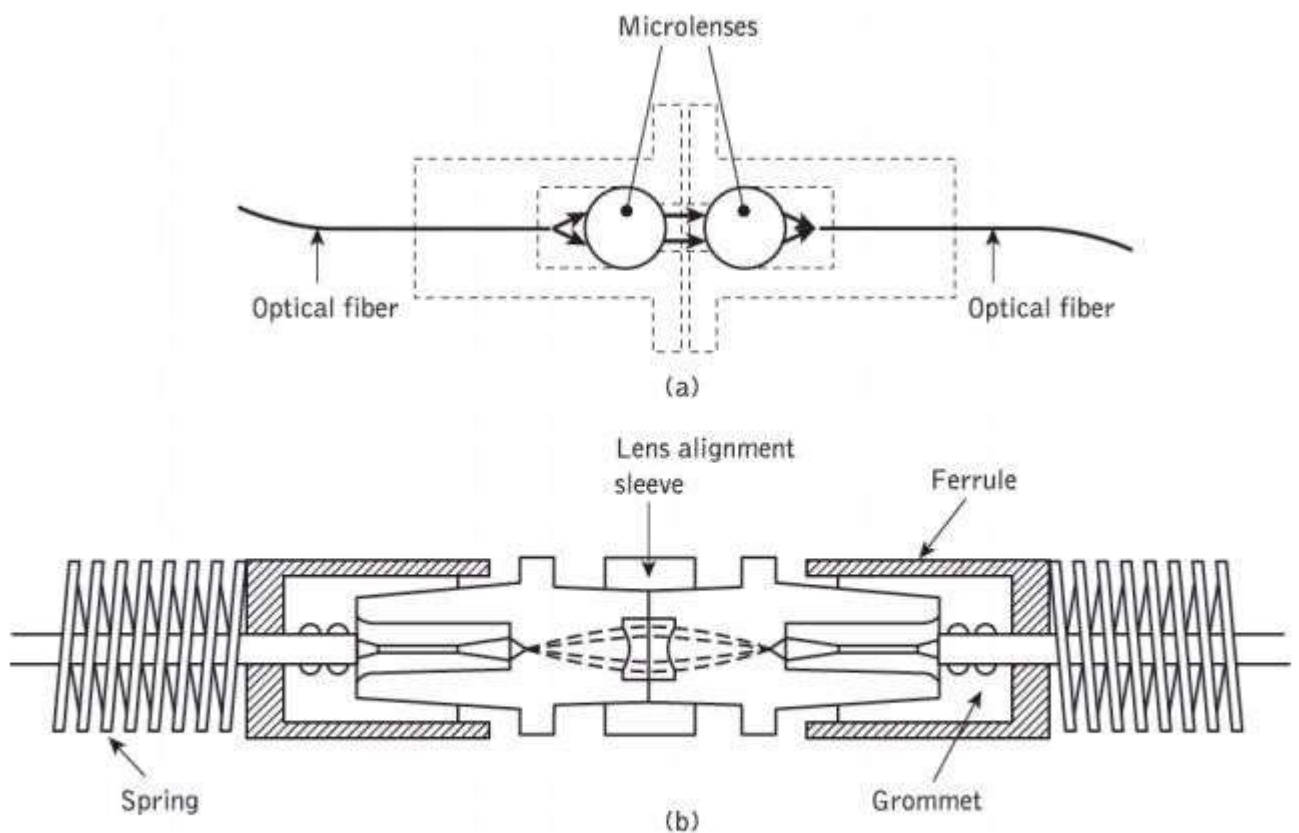


Figure 2.31 Lens-coupled expanded beam connectors: (a) schematic diagram of a connector with two microlenses making a 1:1 image of the emitting fiber upon the receiving one; (b) molded plastic lens connector assembly

[Source: <http://img.brainkart.com>]

Fiber Couplers

An optical fiber coupler is a device that distributes light from a main fiber into one or more branch fibers.* The latter case is more normal and such devices are known as multiport fiber couplers. Requirements are increasing for the use of these devices to divide or combine optical signals for application within optical fiber information distribution systems including data buses, LANs, computer networks and telecommunication access networks.

Optical fiber couplers are often passive devices in which the power transfer takes place either:

- (a) through the fiber core cross-section by butt jointing the fibers or by using some form of imaging optics between the fibers (core interaction type); or
- (b) through the fiber surface and normal to its axis by converting the guided core modes to both cladding and refracted modes which then enable the power-sharing mechanism (surface interaction type).

Multiport optical fiber couplers can also be subdivided into the following three main groups, as illustrated in Figure 2.32.

1. Three- and four-port* couplers, which are used for signal splitting, distribution and combining.
2. Star couplers, which are generally used for distributing a single input signal to multiple outputs.

3. Wavelength division multiplexing (WDM) devices, which are a specialized form of coupler designed to permit a number of different peak wavelength optical signals to be transmitted in parallel on a single fiber.

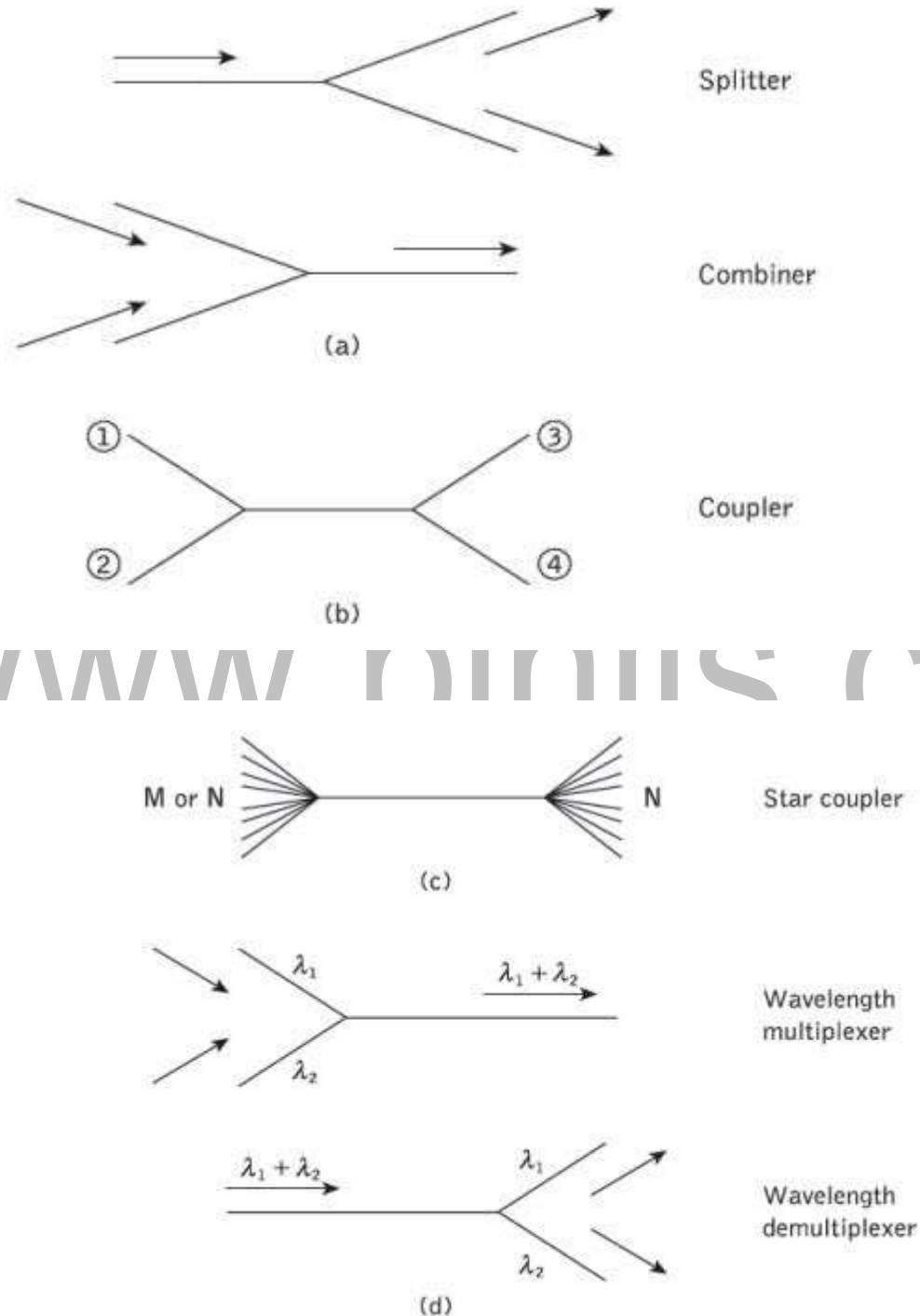


Figure 2.32 Optical fiber coupler types and functions: (a) three-port couplers; (b) four-port coupler; (c) star coupler; (d) wavelength division multiplexing and demultiplexing couplers

[Source: <http://img.brainkart.com>]

In this context WDM couplers either combine the different wavelength optical signal onto the fiber (i.e. multiplex) or separate the different wavelength optical signals output from the fiber (i.e. demultiplex). Ideal fiber couplers should distribute light among the branch fibers with no scattering loss† or the generation of noise, and they should function with complete insensitivity to factors including the distribution of light between the fiber modes, as well as the state of polarization of the light. Unfortunately, in practice passive fiber couplers do not display all of the above properties and hence the characteristics of the devices affect the performance of optical fiber networks. Four-port couplers may also be referred to as 2*2 star couplers.

The scattering loss through the coupler is often referred to as the excess loss.

1. Three- and Four-Port Couplers

Several methods are employed to fabricate three- and four-port optical fiber couplers. The lateral offset method, illustrated in Figure 2.33(a), relies on the overlapping of the fiber end faces. Light from the input fiber is coupled to the output fibers according to the degree of overlap. Hence the input power can be distributed in a welldefined proportion by appropriate control of the amount of lateral offset between the fibers. This technique, which can provide a bidirectional coupling capability, is well suited for use with multimode step index fibers but may incur higher excess losses than other methods as all the input light cannot be coupled into the output fibers.

Another coupling technique is to incorporate a beam splitter element between the fibers. The semitransparent mirror method provides an ingenious way to accomplish such a fiber coupler, as shown in Figure 2.33(b). A partially reflecting surface can be applied directly to the fiber end face cut at an angle of 45° to form a thin-film beam splitter.

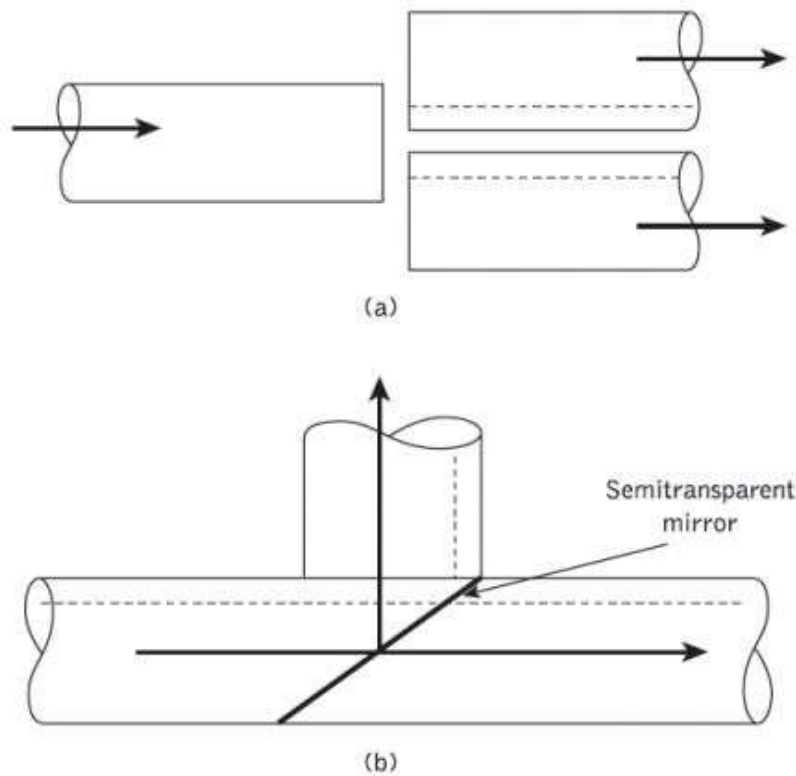


Figure 2.33 Fabrication techniques for three-port fiber couplers: (a) the lateral offset method; (b) the semitransparent mirror method

[Source: <http://img.brainkart.com>]

A fast-growing category of optical fiber coupler is based on the use of micro-optic components. In particular, a complete range of couplers has been developed which utilize the beam expansion and collimation properties of the GRIN-rod lens combined with spherical retro-reflecting mirrors. These devices, two of which are displayed in Figure 2.34, are miniature optical assemblies of compact construction which generally exhibit low insertion loss (typically less than 1 dB) and are insensitive to modal power distribution. Figure 2.34(a) shows the structure of a parallel surface type of GRIN-rod lens three port coupler which comprises two quarter pitch lenses with a semitransparent mirror in between. Light rays from the input fiber $F1$ collimate in the first lens before they are incident on the mirror. A portion of the incident beam is reflected back and is coupled to fiber $F2$, while the transmitted light is focused

in the second lens and then coupled to fiber F_3 . The slant surface version of the similar coupler is shown in Figure 2.34(b). The parallel surface type, however, is the most attractive due to its ease of fabrication, compactness, simplicity and relatively low insertion loss. Finally, the substitution of the mirror by an interference filter* offers application of these devices to WDM

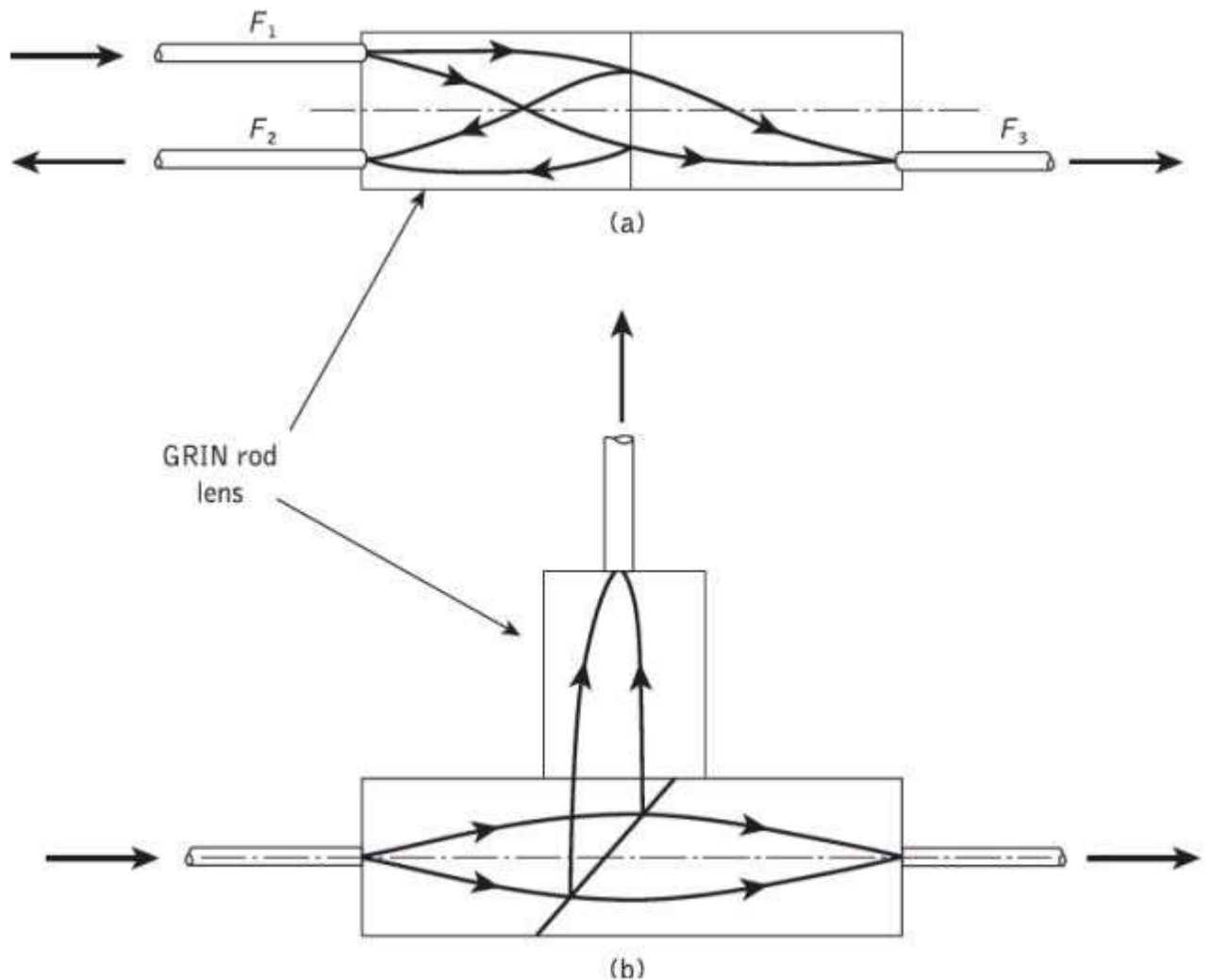


Figure 2.34 GRIN-rod lens micro-optic fiber couplers: (a) parallel surface type; (b) slant surface type

[Source: <http://img.brainkart.com>]

Perhaps the most common method for manufacturing couplers is the fused biconical taper (FBT) technique. In this method the fibers are generally twisted together and then spot fused under tension such that the fused section is elongated to form a biconical taper structure. A three-port coupler is formed

by removing one of the input fibers. Optical power launched into the input fiber propagates in the form of guided core modes.

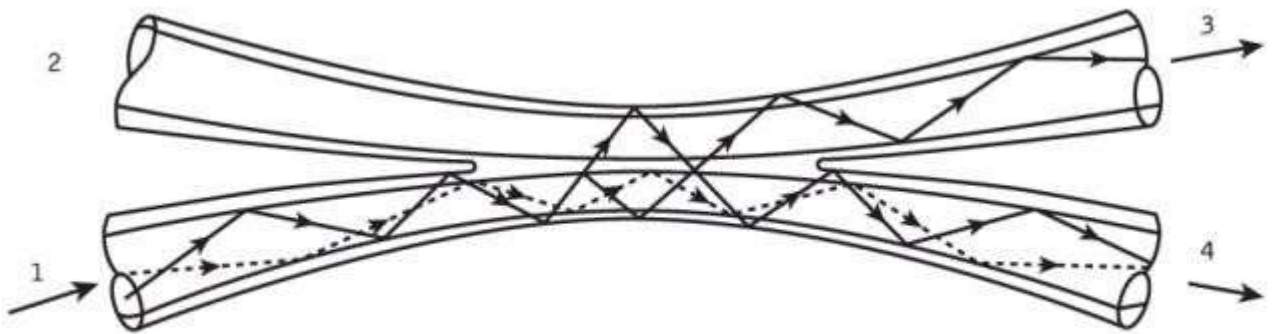


Figure 2.35 Structure and principle of operation for the fiber fused biconical taper coupler

[Source: <http://img.brainkart.com>]

The higher order modes, however, leave the fiber core because of its reduced size in the tapered-down region and are therefore guided as cladding modes. These modes transfer back to guided core modes in the tapered-up region of the output fiber with an approximately even distribution between the two fibers. Often only a portion of the total power is coupled between the two fibers because only the higher order modes take part in the process, the lower order modes generally remaining within the main fiber. In this case a mode-dependent (and therefore wavelength-dependent) coupling ratio is obtained. However, when the waist of the taper is made sufficiently narrow, then the entire mode volume can be encouraged to participate in the coupling process and a larger proportion of input power can be shared between the output fibers. This strategy gives an improvement in both the power and modal uniformity of the coupler. The various loss parameters associated with four-port couplers may be written down with reference to Figure 2.35. Hence, the excess loss which is defined as the ratio of power input to power output is given by:

$$\text{Excess loss (four-port coupler)} = 10 \log_{10} \frac{P_1}{(P_3 + P_4)} \text{ (dB)}$$

$$\text{Insertion loss (ports 1 to 4)} = 10 \log_{10} \frac{P_1}{P_4} \text{ (dB)}$$

$$\text{Crosstalk (four-port coupler)} = 10 \log_{10} \frac{P_2}{P_1} \text{ (dB)}$$

Finally, the splitting or coupling ratio indicates the percentage division of optical power between the output ports. Again referring to Figure 2.35:

$$\begin{aligned} \text{Split ratio} &= \left[\frac{P_3}{(P_3 + P_4)} \right] \times 100\% \\ &= \left[1 - \frac{P_4}{(P_3 + P_4)} \right] \times 100\% \end{aligned}$$

2. Star Couplers

Star couplers distribute an optical signal from a single-input fiber to multiple-output fibers. The two principal manufacturing techniques for producing multimode fiber star couplers are the mixer-rod and the FBT methods. In the mixer-rod method illustrated in Figure 2.36 a thin platelet of glass is employed, which effectively mixes the light from one fiber, dividing it among the outgoing fibers. This method can be used to produce a transmissive star coupler or a reflective star coupler, as displayed in Figure 2.36. The typical insertion loss for an 8 * 8 mixer-rod transmissive star coupler with fiber pigtails is 12.5 dB with port-to-port uniformity of ± 0.7 dB.

Thus the fibers which constitute the star coupler are bundled, twisted, heated and pulled, to form the device illustrated in Figure. 2.37. With multimode fiber this method relies upon the coupling of higher order modes between the different fibers. It is therefore highly mode dependent, which results in a

relatively wide port-to-port output variation in comparison with star couplers based on the mixer-rod technique. In an ideal star coupler the optical power from any input fiber is evenly distributed among the output fibers. The total loss associated with the star coupler comprises its theoretical splitting loss together with the excess loss. The splitting loss is related to the number of output ports N following:

$$\text{Splitting loss (star coupler)} = 10 \log_{10} N \text{ (dB)}$$

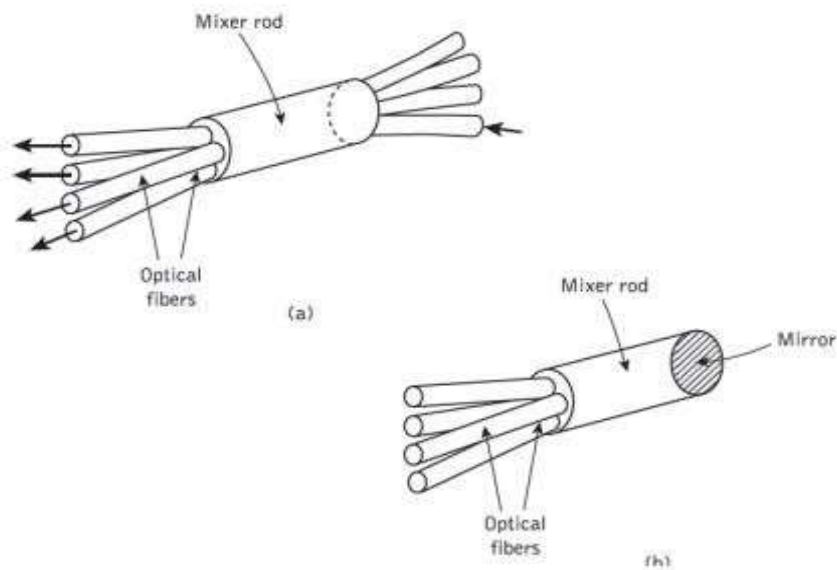


Figure 2.36 Fiber star couplers using the mixer-rod technique: (a) transmissive star coupler; (b) reflective star coupler

[Source: <http://img.brainkart.com>]

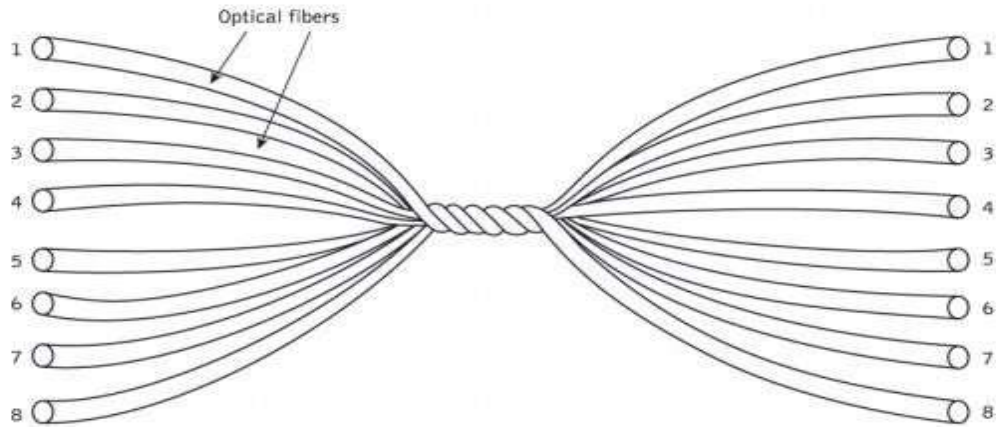


Figure 2.37 Fiber fused biconical taper 8 × 8 port star coupler

For a single input port and multiple output ports where $j = 1, N$, then the excess loss is given by:

$$\text{Excess loss (star coupler)} = 10 \log_{10} \left(P_i / \sum_1^N P_j \right) \text{ (dB)}$$

[Source: <http://img.brainkart.com>]

www.binils.com

Fiber Alignment and Joint Loss

A major consideration with all types of fiber–fiber connection is the optical loss encountered at the interface. Even when the two jointed fiber ends are smooth and perpendicular to the fiber axes, and the two fiber axes are perfectly aligned, a small proportion of the light may be reflected back into the transmitting fiber causing attenuation at the joint. This phenomenon, known as Fresnel reflection, is associated with the step changes in refractive index at the jointed interface (i.e. glass–air–glass). The magnitude of this partial reflection of the light transmitted through the interface may be estimated using the classical Fresnel formula for light of normal incidence and is given by

$$r = \left(\frac{n_1 - n}{n_1 + n} \right)^2 \quad (2.59)$$

where r is the fraction of the light reflected at a single interface, n_1 is the refractive index of the fiber core and n is the refractive index of the medium between the two jointed fibers (i.e. for air $n = 1$). However, in order to determine the amount of light reflected at a fiber joint, Fresnel reflection at both fiber interfaces must be taken into account. The loss in decibels due to Fresnel reflection at a single interface is given by:

$$\text{Loss}_{\text{Fres}} = -10 \log_{10}(1 - r) \quad (2.60)$$

Hence, using the relationships given in Eqs (2.59) and (2.60) it is possible to determine the optical attenuation due to Fresnel reflection at a fiber–fiber joint.

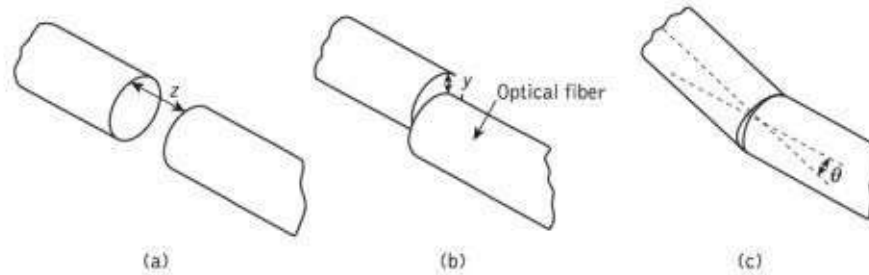


Figure 2.17 The three possible types of misalignment which may occur when jointing compatible optical fibers: (a) longitudinal misalignment; (b) lateral misalignment; (c) angular misalignment

[Source: <http://img.brainkart.com>]

It is apparent that Fresnel reflection may give a significant loss at a fiber joint even when all other aspects of the connection are ideal. However, the effect of Fresnel reflection at a fiber–fiber connection can be reduced to a very low level through the use of an index-matching fluid in the gap between the jointed fibers. When the index-matching fluid has the same refractive index as the fiber core, losses due to Fresnel reflection are in theory eradicated. Unfortunately, Fresnel reflection is only one possible source of optical loss at a fiber joint. A potentially greater source of loss at a fiber–fiber connection is caused by misalignment of the two jointed fibers. In order to appreciate the development and relative success of various connection techniques it is useful to discuss fiber alignment in greater detail.

Any deviations in the geometrical and optical parameters of the two optical fibers which are jointed will affect the optical attenuation (insertion loss) through the connection. It is not possible within any particular connection technique to allow for all these variations. Hence, there are inherent connection problems when jointing fibers with, for instance

- ✓ different core and/or cladding diameters;
- ✓ different numerical apertures and/or relative refractive index differences;
- ✓ different refractive index profiles;

✓ fiber faults (core ellipticity, core concentricity, etc.).

The losses caused by the above factors together with those of Fresnel reflection are usually referred to as intrinsic joint losses. The best results are therefore achieved with compatible (same) fibers which are manufactured to the lowest tolerance.

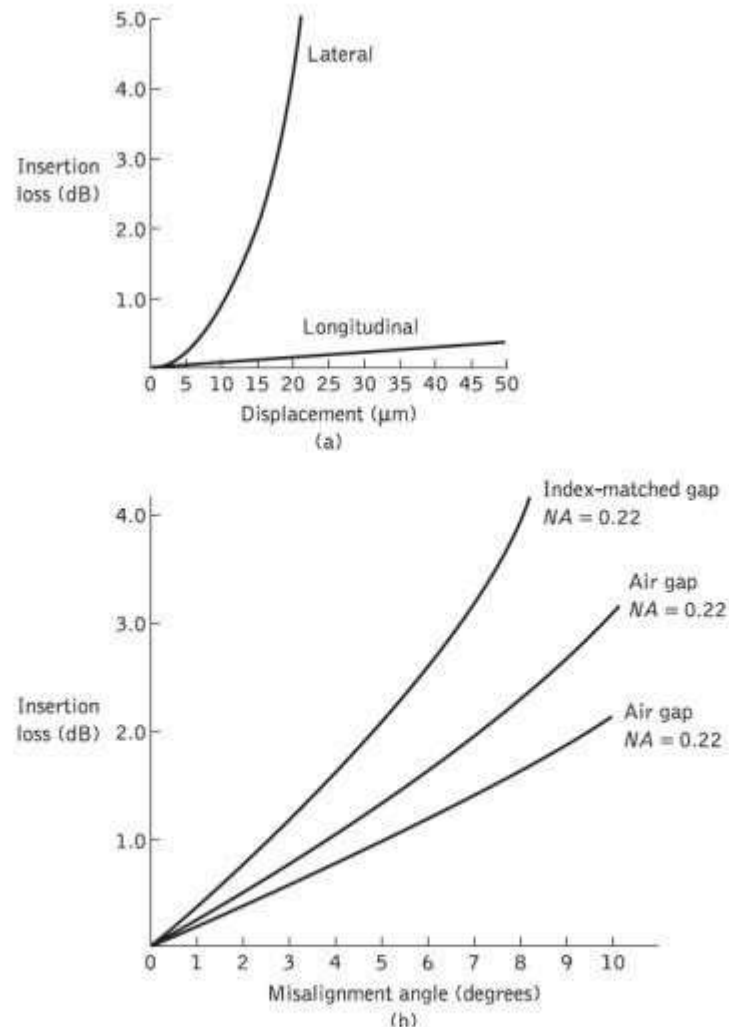


Figure 2.18 Insertion loss characteristics for jointed optical fibers with various types of misalignment: (a) insertion loss due to lateral and longitudinal misalignment for a graded index fiber of 50 μm core diameter.

[Source: <http://img.brainkart.com>]

In this case there is still the problem of the quality of the fiber alignment provided by the jointing mechanism. Examples of possible misalignment between coupled compatible optical fibers are illustrated in Figure 2.17. It is

apparent that misalignment may occur in three dimensions: the separation between the fibers (longitudinal misalignment), the offset perpendicular to the fiber core axes (lateral/radial/axial misalignment) and the angle between the core axes (angular misalignment).

Optical losses resulting from these three types of misalignment depend upon the fiber type, core diameter and the distribution of the optical power between the propagating modes. Examples of the measured optical losses due to the various types of misalignment are shown in Figure 2.18. Figure 2.18(a) shows the attenuation characteristic for both longitudinal and lateral misalignment of a graded index fiber of 50 μm core diameter.

It may be observed that the lateral misalignment gives significantly greater losses per unit displacement than the longitudinal misalignment. For instance, in this case a lateral displacement of 10 μm gives about 1 dB insertion loss whereas a similar longitudinal displacement gives an insertion loss of around 0.1 dB. Figure 2.18(b) shows the attenuation characteristic for the angular misalignment of two multimode step index fibers with numerical apertures of 0.22 and 0.3. An insertion loss of around 1 dB is obtained with angular misalignment of 4° and 5° for the $NA=0.22$ and $NA=0.3$ fibers respectively.

It may also be observed in Figure 2.18(b) that the effect of an index-matching fluid in the fiber gap causes increased losses with angular misalignment. Therefore, it is clear that relatively small levels of lateral and/or angular misalignment can cause significant attenuation at a fiber joint. This is especially the case for fibers of small core diameter (less than 150 μm) which are currently employed for most telecommunication purposes.

1. Multimode Fiber Joints

Theoretical and experimental studies of fiber misalignment in optical fiber connections allow approximate determination of the losses encountered with the various misalignments of different fiber types. We consider here some of the expressions used to calculate losses due to lateral and angular misalignment of optical fiber joints. Longitudinal misalignment is not discussed in detail as it tends to be the least important effect and may be largely avoided in fiber connection.

Both groups of workers claim good agreement with experimental results, which is perhaps understandable when considering the number of variables involved in the measurement. Also, all groups predict higher losses for fibers with larger numerical apertures, which is consistent with intuitive considerations (i.e. the larger the numerical aperture, the greater the spread of the output light and the higher the optical loss at a longitudinally misaligned joint).

Theoretical expressions for the determination of lateral and angular misalignment losses are by no means definitive, although in all cases they claim reasonable agreement with experimental results. However, experimental results from different sources tend to vary (especially for angular misalignment losses) due to difficulties of measurement. It is therefore not implied that the expressions given in the text are necessarily the most accurate, as at present the choice appears somewhat arbitrary. Lateral misalignment reduces the overlap region between the two fiber cores. Assuming uniform excitation of all the optical modes in a multimode step index fiber, the overlapped area between both fiber cores approximately gives the lateral coupling efficiency

μ_{lat} . Hence, the lateral coupling efficiency for two similar step index fibers may be written as

$$\eta_{lat} \approx \frac{16(n_1/n)^2}{[1 + (n_1/n)]^4} \frac{1}{\pi} \left\{ 2 \cos^{-1} \left(\frac{y}{2a} \right) - \left(\frac{y}{a} \right) \left[1 - \left(\frac{y}{2a} \right)^2 \right]^{\frac{1}{2}} \right\} \quad (2.61)$$

where n_1 is the core refractive index, n is the refractive index of the medium between the fibers, y is the lateral offset of the fiber core axes, and a is the fiber core radius. The lateral misalignment loss in decibels may be determined using:

$$\text{Loss}_{lat} = -10 \log_{10} \eta_{lat} \text{ dB} \quad (2.62)$$

The predicted losses obtained using the formulas given in Eqs (2.61) and (2.62) are generally slightly higher than the measured values due to the assumption that all modes are equally excited. This assumption is only correct for certain cases of optical fiber transmission. Also, certain authors assume index matching and hence no Fresnel reflection, which makes the first term in Eq. (2.61) equal to unity (as $n_1/n = 1$). This may be valid if the two fiber ends are assumed to be in close contact (i.e. no air gap in between) and gives lower predicted losses. Nevertheless, bearing in mind these possible inconsistencies, useful estimates for the attenuation due to lateral misalignment of multimode step index fibers may be obtained. Lateral misalignment loss in multimode graded index fibers assuming a uniform distribution of optical power throughout all guided modes was calculated by Gloge. He estimated that the lateral misalignment loss was dependent on the refractive index gradient α for small lateral offset and may be obtained from:

$$L_1 = \frac{2}{\pi} \left(\frac{y}{a} \right) \left(\frac{\alpha + 2}{\alpha + 1} \right) \quad \text{for } 0 \leq y \leq 0.2a \quad (2.63)$$

where the lateral coupling efficiency was given by:

$$\eta_{\text{lat}} = 1 - L_1 \quad (2.64)$$

Hence Eq. (2.64) may be utilized to obtain the lateral misalignment loss in decibels. With a parabolic refractive index profile where $\alpha = 2$, Eq. (2.63) gives:

$$L_1 = \frac{8}{3\pi} \left(\frac{y}{a} \right) = 0.85 \left(\frac{y}{a} \right) \quad (2.65)$$

A further estimate including the leaky modes gave a revised expression for the lateral misalignment loss given in Eq. (2.64) of $0.75(y/a)$. This analysis was also extended to step index fibers (where $\alpha = \infty$) and gave lateral misalignment losses of $0.64(y/a)$ and $0.5(y/a)$ for the cases of guided modes only and both guided plus leaky modes respectively.

Factors causing fiber–fiber intrinsic losses were listed in previous Section; the major ones comprising a mismatch in the fiber core diameters, a mismatch in the fiber numerical apertures and differing fiber refractive index profiles are illustrated in Figure 2.19. Connections between multimode fibers with certain of these parameters being different can be quite common, particularly when a pigtailed optical source is used, the fiber pigtail of which has different characteristics from the main transmission fiber. Moreover, as indicated previously, diameter variations can occur with the same fiber type.

Assuming all the modes are equally excited in a multimode step or graded index fiber, and that the numerical apertures and index profiles are the same, then the loss resulting from a mismatch of core diameters (see Figure 2.19(a)) is given by:

$$\text{Loss}_{\text{cb}} = \begin{cases} -10 \log_{10} \left(\frac{a_2}{a_1} \right)^2 \text{ (dB)} & a_2 < a_1 \\ 0 & a_2 \geq a_1 \end{cases} \quad (2.66)$$

where a_1 and a_2 are the core radii of the transmitting and receiving fibers respectively. It may be observed from Eq. (2.66) that no loss is incurred if the receiving fiber has a larger core diameter than the transmitting one. In addition, only a relatively small loss (0.09 dB) is obtained when the receiving fiber core diameter is 1% smaller than that of the transmitting fiber.

When the transmitting fiber has a higher numerical aperture than the receiving fiber, then some of the emitted light rays will fall outside the acceptance angle of the receiving fiber and they will therefore not be coupled through the joint. Again assuming a uniform modal power distribution, and fibers with equivalent refractive index profiles and core diameters, then the loss caused by a mismatch of numerical apertures (see Figure 2.19(b))

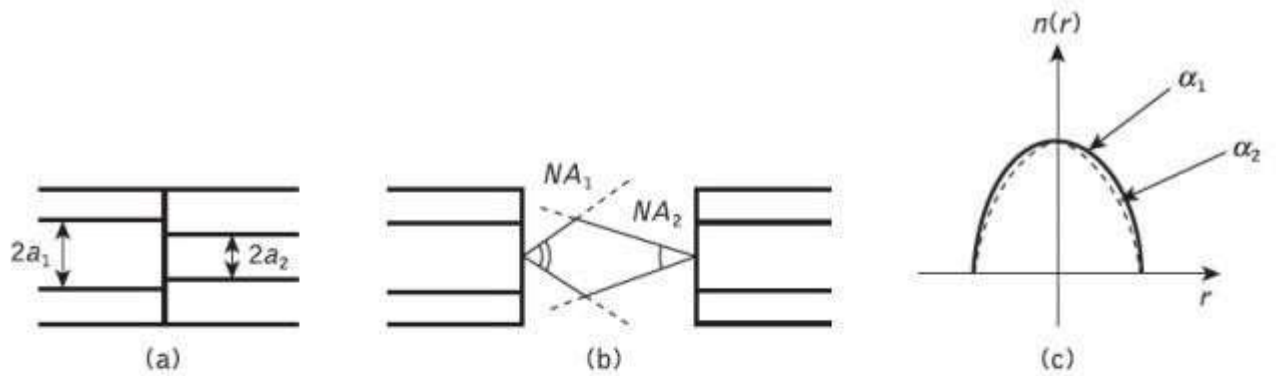


Figure 2.19 Some intrinsic coupling losses at fiber joints: (a) core diameter mismatch; (b) numerical aperture mismatch; (c) refractive index profile difference

$$\text{Loss}_{\text{NA}} = \begin{cases} -10 \log_{10} \left(\frac{NA_2}{NA_1} \right)^2 \text{ (dB)} & NA_2 < NA_1 \\ 0 & \text{(dB)} \quad NA_2 \geq NA_1 \end{cases} \quad (2.67)$$

$$\text{Loss}_{\text{RI}} = \begin{cases} -10 \log_{10} \frac{\alpha_2(\alpha_1 + 2)}{\alpha_1(\alpha_2 + 2)} \text{ (dB)} & \alpha_2 < \alpha_1 \\ 0 & \text{(dB)} \quad \alpha_2 \geq \alpha_1 \end{cases} \quad (2.68)$$

$$\text{Loss}_{\text{int}} = \begin{cases} -10 \log_{10} \frac{(a_2 NA_2)^2 (\alpha_1 + 2) \alpha_2}{(a_1 NA_1)^2 (\alpha_2 + 2) \alpha_1} \text{ (dB)} & a_2 > a_1, NA_2 > NA_1, \alpha_2 > \alpha_1 \\ 0 & \text{(dB)} \quad a_2 \leq a_1, NA_2 \leq NA_1, \alpha_2 \leq \alpha_1 \end{cases} \quad (2.67)$$

[Source: <http://img.brainkart.com>]

2. Single-Mode Fiber Joints

Misalignment losses at connections in single-mode fibers have been theoretically considered by Marcuse and Gambling *et al.* The theoretical analysis which was instigated by Marcuse is based upon the Gaussian or near-Gaussian shape of the modes propagating in single-mode fibers regardless of the fiber type (i.e. step index or graded index). Further development of this theory by Gambling *et al.* gave simplified formulas for both the lateral and angular misalignment losses at joints in single mode fibers. In the absence of angular misalignment Gambling *et al.* calculated that the loss \mathcal{T} due to lateral offset y was given by:

$$T_1 = 2.17 \left(\frac{y}{\omega} \right)^2 \text{ dB} \quad (2.68)$$

where ω is the normalized spot size of the fundamental mode.* However, the normalized spot size for the LP01 mode (which corresponds to the HE mode) may be obtained from the empirical formula:

$$\omega = a \frac{(0.65 + 1.62 V^{-3/2} + 2.88 V^{-6})}{2^{1/2}} \quad (2.69)$$

where ω is the spot size in μm , a is the fiber core radius and V is the normalized frequency for the fiber. Alternatively, the insertion loss T_a caused by an angular misalignment θ (in radians) at a joint in a single-mode fiber may be given by

$$T_a = 2.17 \left(\frac{\theta \omega n_1 V}{a NA} \right)^2 \text{ dB} \quad (2.70)$$

where n_1 is the fiber core refractive index and NA is the numerical aperture of the fiber. It must be noted that the formulas given in Eqs (2.69) and (2.70) assume that the spot sizes of the modes in the two coupled fibers are the same. Gambling *et al.* also derived a somewhat complicated formula which gave a good approximation for the combined losses due to both lateral and angular misalignment at a fiber joint. However, they indicate that for small total losses (less than 0.75 dB) a reasonable approximation is obtained by simply combining Eqs (2.68) and (2.70). Assuming that no losses are present due to the extrinsic factors, the intrinsic coupling loss is given by

$$\text{Loss}_{\text{int}} = -10 \log_{10} \left[4 \left(\frac{\omega_{02}}{\omega_{01}} + \frac{\omega_{01}}{\omega_{02}} \right)^{-2} \right] \text{ (dB)} \quad (2.71)$$

where ω_{01} and ω_{02} are the spot sizes of the transmitting and receiving fibers respectively. Equation (2.71) therefore enables the additional coupling loss resulting from mode-field diameter mismatch between two single-mode fibers to be calculated.

www.binils.com

Fiber Splices

A permanent joint formed between two individual optical fibers in the field or factory is known as a fiber splice. Fiber splicing is frequently used to establish long-haul optical fiber links where smaller fiber lengths need to be joined, and there is no requirement for repeated connection and disconnection. Splices may be divided into two broad categories depending upon the splicing technique utilized. These are fusion splicing or welding and mechanical splicing.

Fusion splicing is accomplished by applying localized heating (e.g. by a flame or an electric arc) at the interface between two butted, prealigned fiber ends causing them to soften and fuse. Mechanical splicing, in which the fibers are held in alignment by some mechanical means, may be achieved by various methods including the use of tubes around the fiber ends (tube splices) or V-grooves into which the butted fibers are placed (groove splices). All these techniques seek to optimize the splice performance (i.e. reduce the insertion loss at the joint) through both fiber end preparation and alignment of the two joint fibers. Typical average splice insertion losses for multimode fibers are in the range 0.1 to 0.2 dB which is generally a better performance than that exhibited by demountable connections.

It may be noted that the insertion losses of fiber splices are generally much less than the possible Fresnel reflection loss at a butted fiber–fiber joint. This is because there is no large step change in refractive index with the fusion splice as it forms a continuous fiber connection, and some method of index matching (e.g. a fluid) tends to be utilized with mechanical splices

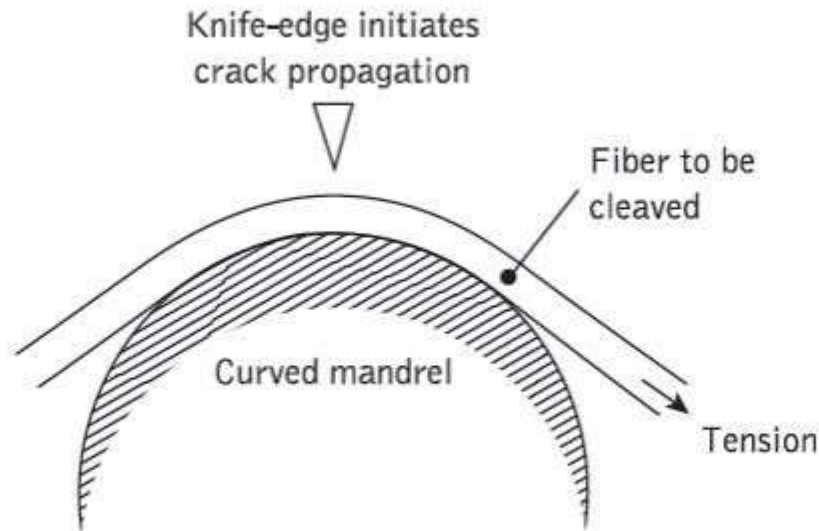


Figure 2.20 Optical fiber end preparation: the principle of scribe and break cutting

[Source: <http://img.brainkart.com>]

A requirement with fibers intended for splicing is that they have smooth and square end faces. In general this end preparation may be achieved using a suitable tool which cleaves the fiber as illustrated in Figure 2.20. This process is often referred to as scribe and break or score and break as it involves the scoring of the fiber surface under tension with a cutting tool (e.g. sapphire, diamond, tungsten carbide blade). The surface scoring creates failure as the fiber is tensioned and a clean, reasonably square fiber end can be produced. Figure 2.20 illustrates this process with the fiber tensioned around a curved mandrel. However, straight pull, scribe and break tools are also utilized, which arguably give better results.

1. Fusion Splices

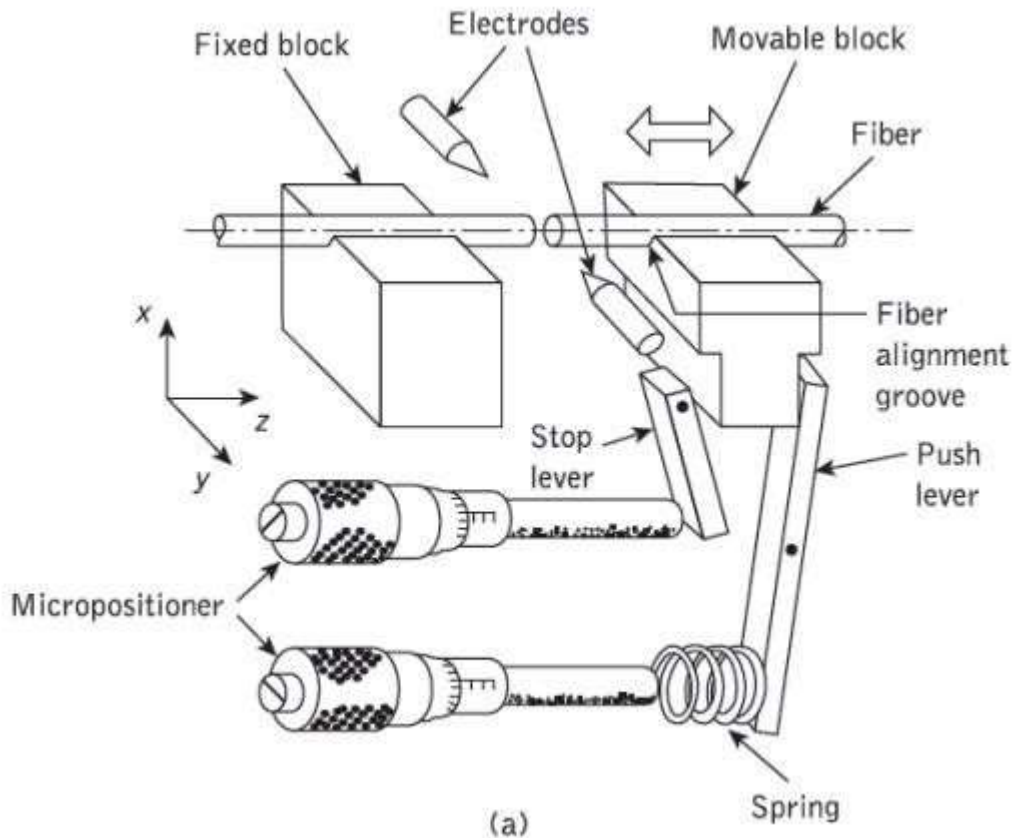
The fusion splicing of single fibers involves the heating of the two prepared fiber ends to their fusing point with the application of sufficient axial pressure between the two optical fibers. It is therefore essential that the stripped (of

cabling and buffer coating) fiber ends are adequately positioned and aligned in order to achieve good continuity of the transmission medium at the junction point. Hence the fibers are usually positioned and clamped with the aid of an inspection microscope.

Flame heating sources such as microplasma torches (argon and hydrogen) and oxyhydrogen microburners (oxygen, hydrogen and alcohol vapor) have been utilized with some success. However, the most widely used heating source is an electric arc. This technique offers advantages of consistent, easily controlled heat with adaptability for use under field conditions.

A schematic diagram of the basic arc fusion method is given in Figure 2.21(a) illustrating how the two fibers are welded together. Figure 2.21(b) shows a development of the basic arc fusion process which involves the rounding of the fiber ends with a low-energy discharge before pressing the fibers together and fusing with a stronger arc.

This technique, known as pre-fusion, removes the requirement for fiber end preparation which has a distinct advantage in the field environment. It has been utilized with multimode fibers giving average splice losses of 0.09 db.



[Source: <http://img.brainkart.com>]

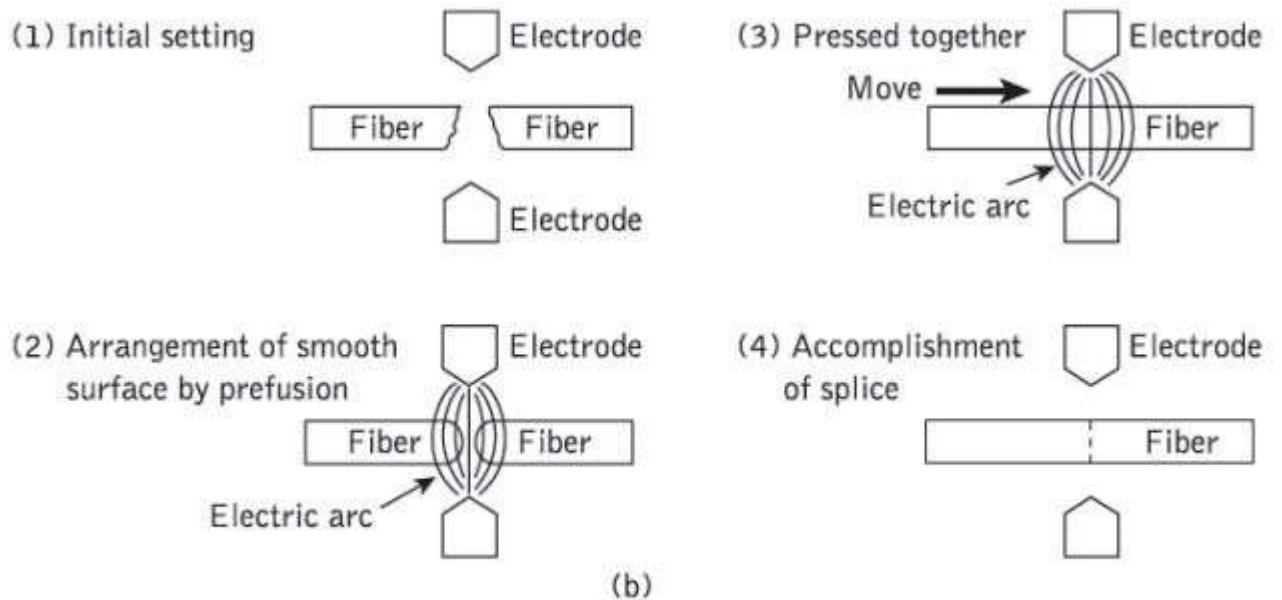


Figure 2.21 Electric arc fusion splicing: (a) an example of fusion splicing apparatus; (b) schematic illustration of the prefusion method for accurately splicing optical fibers

[Source: <http://img.brainkart.com>]

Fusion splicing of single-mode fibers with typical core diameters between 5 and 10 μm presents problems of more critical fiber alignment (i.e. lateral offsets of less than 1 μm are required for low loss joints). However, splice insertion losses below 0.3 dB may be achieved due to a self-alignment phenomenon which partially compensates for any lateral offset.

Self-alignment, illustrated in Figure 2.22, is caused by surface tension effects between the two fiber ends during fusing. An early field trial of single-mode fiber fusion splicing over a 31.6 km link gave mean splice insertion losses of 0.18 and 0.12 dB at wavelengths of 1.3 and 1.55 μm respectively. Mean splice losses of only 0.06 dB have also been obtained with a fully automatic single-mode fiber fusion splicing machine weaken the fiber in the vicinity of the splice. It has been found that even with careful handling, the tensile strength of the fused fiber may be as low as 30% of that of the uncoated fiber before fusion.

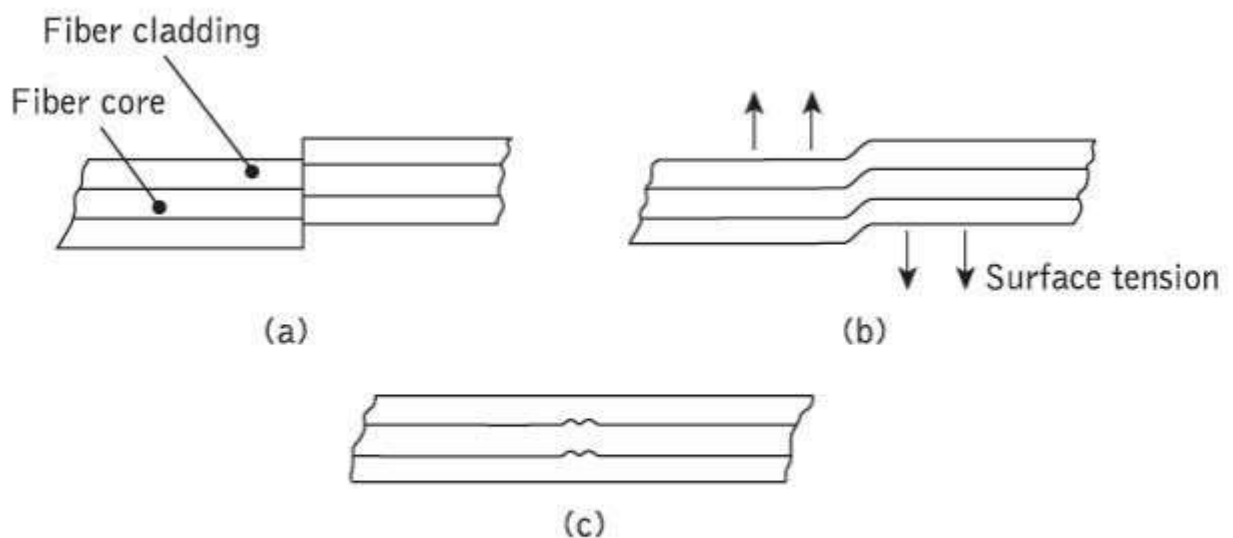


Figure 2.22 Self-alignment phenomenon which takes place during fusion splicing: (a) before fusion; (b) during fusion; (c) after fusion

[Source: <http://img.brainkart.com>]

The fiber fracture generally occurs in the heat affected zone adjacent to the fused joint. The reduced tensile strength is attributed to the combined effects of surface damage caused by handling, surface defect growth during heating and induced residual stresses due to changes in chemical composition. It is therefore necessary that the completed splice is packaged so as to reduce tensile loading upon the fiber in the vicinity of the splice.

2. Mechanical Splices

A number of mechanical techniques for splicing individual optical fibers have been developed. A common method involves the use of an accurately produced rigid alignment tube into which the prepared fiber ends are permanently bonded. This snug tube splice is illustrated in Figure 2.23(a) and may utilize a glass or ceramic capillary with an inner diameter just large enough to accept the optical fibers. Transparent adhesive (e.g. epoxy resin) is injected through a transverse bore in the capillary to give mechanical sealing and index matching of the splice. Average insertion losses as low as 0.1 dB have been obtained with multimode graded index and single-mode fibers using ceramic capillaries. However, in general, snug tube splices exhibit problems with capillary tolerance requirements. Hence as a commercial product they may exhibit losses of up to 0.5 dB.

Mechanical splicing technique which avoids the critical tolerance requirements of the snug tube splice is shown in Figure 2.23(b). This loose tube splice uses an oversized square-section metal tube which easily accepts the prepared fiber ends. Transparent adhesive is first inserted into the tube followed by the fibers. The splice is self-aligning when the fibers are curved in the same plane, forcing the fiber ends simultaneously into the same corner of the tube, as

indicated in Figure 2.23(b). Mean splice insertion losses of 0.073 dB have been achieved using multimode graded index fibers with the loose tube approach.

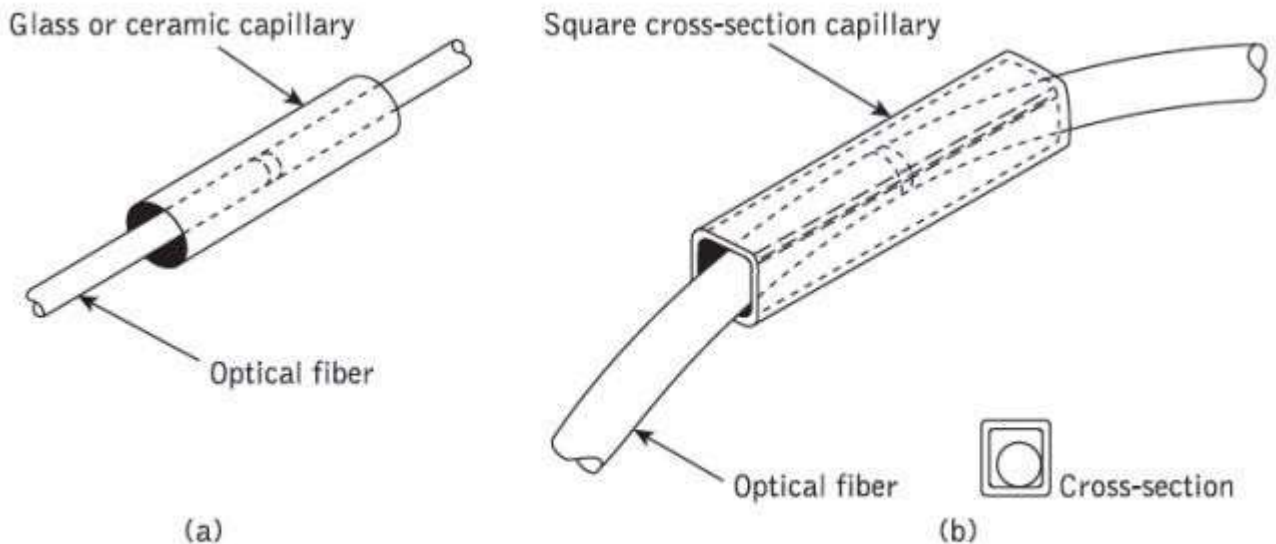


Figure 2.23 Techniques for tube splicing of optical fibers: (a) snug tube splice; (b) loose tube splice utilizing square cross-section capillary

[Source: <http://img.brainkart.com>]

Other common mechanical splicing techniques involve the use of grooves to secure the fibers to be jointed. A simple method utilizes a V-groove into which the two prepared fiber ends are pressed. The V-groove splice which is illustrated in Figure 2.24(a) gives alignment of the prepared fiber ends through insertion in the groove. The splice is made permanent by securing the fibers in the V-groove with epoxy resin. Jigs for producing V-groove splices have proved quite successful, giving joint insertion losses of around 0.1 dB

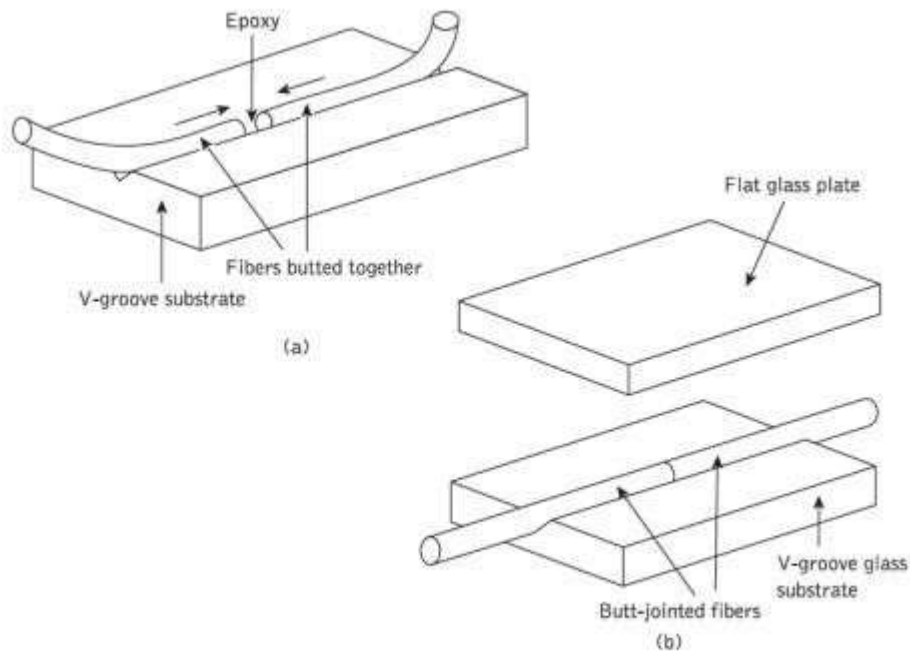


Figure 2.24 V-groove splices

[Source: <http://img.brainkart.com>]

V-groove splices formed by sandwiching the butted fiber ends between a V-groove glass substrate and a flat glass retainer plate, as shown in Figure 2.24(b), have also proved very successful in the laboratory. Splice insertion losses of less than 0.01 dB when coupling single-mode fibers have been reported using this technique. However, reservations are expressed regarding the field implementation of these splices with respect to manufactured fiber geometry, and housing of the splice in order to avoid additional losses due to local fiber bending.

A further variant on the V-groove technique is the elastic tube or elastomeric splice shown in Figure 2.25. The device comprises two elastomeric internal parts, one of which contains a V-groove. An outer sleeve holds the two elastic parts in compression to ensure alignment of the fibers in the V-groove, and fibers with different diameters tend to be centered and hence may be successfully spliced. Although originally intended for multimode fiber connection, the device has become a widely used commercial product which is

employed with single-mode fibers, albeit often as a temporary splice for laboratory investigations. The splice loss for the elastic tube device was originally reported as 0.12 dB or less but is generally specified as around 0.25 dB for the commercial product. In addition, index-matching gel is normally employed within the device to improve its performance.

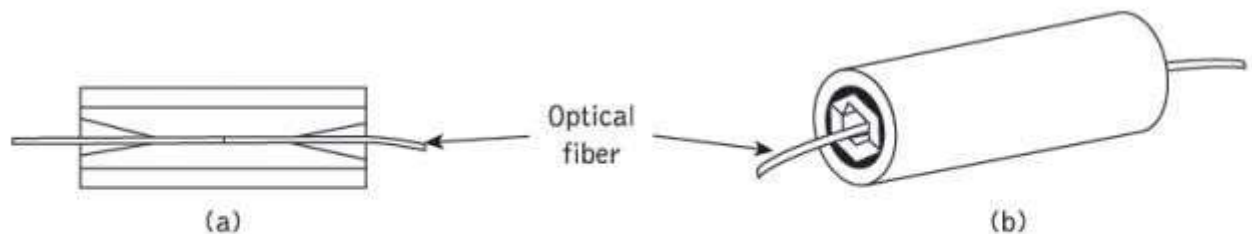


Figure 2.25 The elastomeric splice: (a) cross-section; (b) assembly

[Source: <http://img.brainkart.com>]

A slightly more complex groove splice known as the Springroove® splice utilized a bracket containing two cylindrical pins which serve as an alignment guide for the two prepared fiber ends. The cylindrical pin diameter was chosen to allow the fibers to protrude above the cylinders, as shown in Figure 2.26(a). An elastic element (a spring) was used to press the fibers into a groove and maintain the fiber end alignment, as illustrated in Figure 2.26(b). The complete assembly was secured using a drop of epoxy resin. Mean splice insertion losses of 0.05 dB were obtained using multimode graded index fibers with the Springroove splice. This device found practical use in Italy.

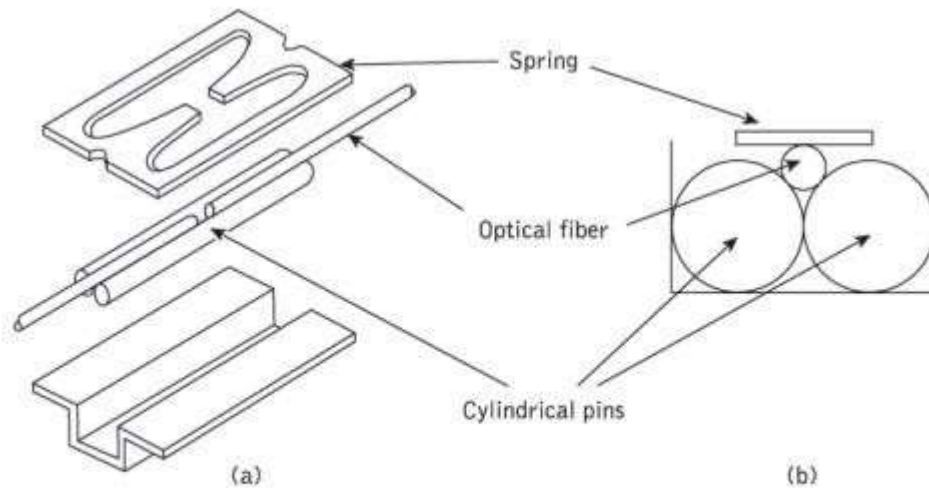


Figure 2.26 The Springgroove splice: (a) expanded overview of the splice, (b) schematic cross-section of the splice

[Source: <http://img.brainkart.com>]

An example of a secondary aligned mechanical splice for multimode fiber is shown in Figure 2.27. This device uses precision glass capillary tubes called ferrules as the secondary elements with an alignment sleeve of metal or plastic into which the glass tubed fibers are inserted. Normal assembly of the splice using 50 μm core diameter fiber yields an average loss of around 0.2 dB.

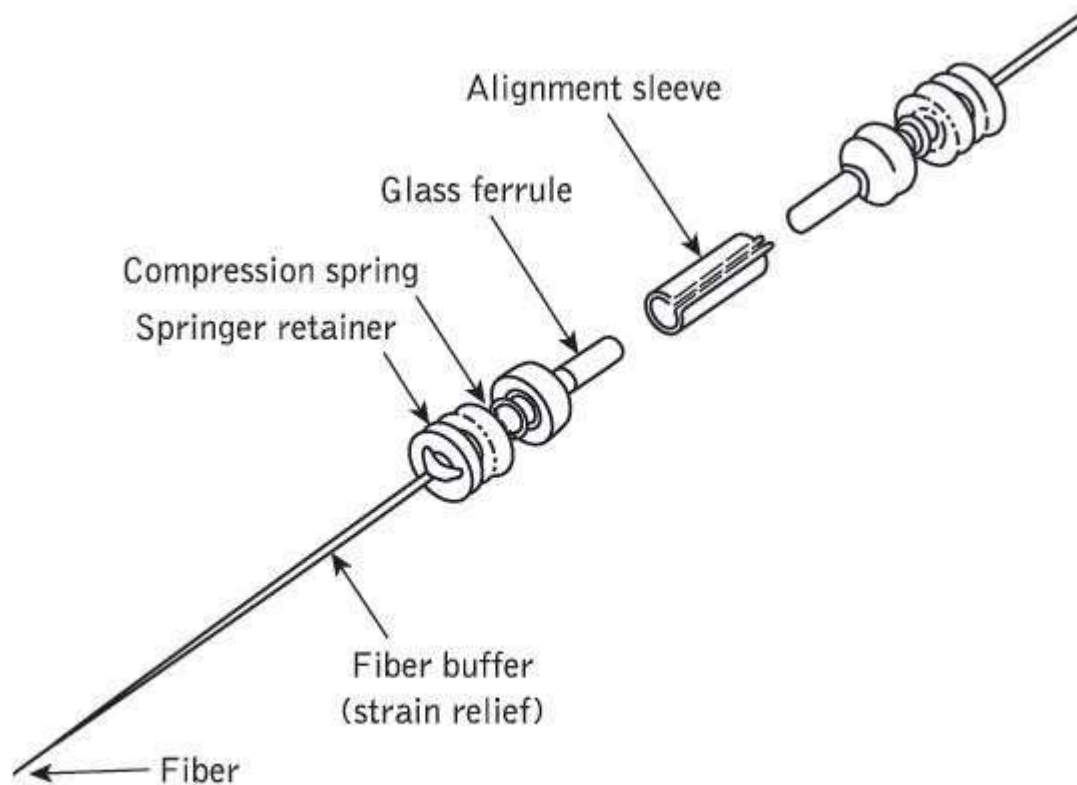


Figure 2.27 Multimode fiber mechanical splice using glass capillary tubes

[Source: <http://img.brainkart.com>]

3. Multiple Splices

Multiple simultaneous fusion splicing of an array of fibers in a ribbon cable has been demonstrated for both multimode and single-mode fibers. In both cases a 12-fiber ribbon was prepared by scoring and breaking prior to pressing the fiber ends onto a contact plate to avoid difficulties with varying gaps between the fibers to be fused.

An electric arc fusing device was then employed to provide simultaneous fusion. Such a device is now commercially available to allow the splicing of 12 fibers simultaneously in a time of around 6 minutes, which requires only 30 seconds per splice. Splice losses using this device with multimode graded index fiber range from an average of 0.04 dB to a maximum of 0.12 dB, whereas for single-mode fiber the average loss is 0.04 dB with a 0.4 dB maximum.

A simple technique employed for multiple simultaneous splicing involves mechanical splicing of an array of fibers, usually in a ribbon cable. The V-groove multiple-splice secondary element comprising etched silicon chips has been used extensively in the United States for splicing multimode fibers. In this technique a 12-fiber splice is prepared by stripping the ribbon and coating material from the fibers. Then the 12 fibers are laid into the trapezoidal* grooves of a silicon chip using a comb structure, as shown in Figure 2.28. The top silicon chip is then positioned prior to applying epoxy to the chip–ribbon interface. Finally, after curing, the front end face is ground and polished.

The process is normally carried out in the factory and the arrays are clipped together in the field, putting index-matching silica gel between the fiber ends. The average splice loss obtained with this technique in the field is 0.12 dB, with the majority of the loss resulting from intrinsic fiber mismatch. Major advantages of this method are the substantial reduction in splicing time (by more than a factor of 10) per fiber and the increased robustness of the final connection. Although early array splicing investigations using silicon chips demonstrated the feasibility of connecting 12*12 fiber arrays, in practice only single 12-fiber ribbons have been spliced at one time due to concerns in relation to splice tolerance and the large number of telecommunication channels which would be present in the two-dimensional array.

An alternative V-groove flat chip molded from a glass-filled polymer resin has been employed in France. Moreover, direct mass splicing of 12-fiber ribbons has also been accomplished. In this technique simultaneous end preparation of all 24 fibers was achieved using a ribbon grinding and polishing procedure. The ribbons were then laid in guides and all 12 fibers were positioned in grooves in the glass-filled plastic

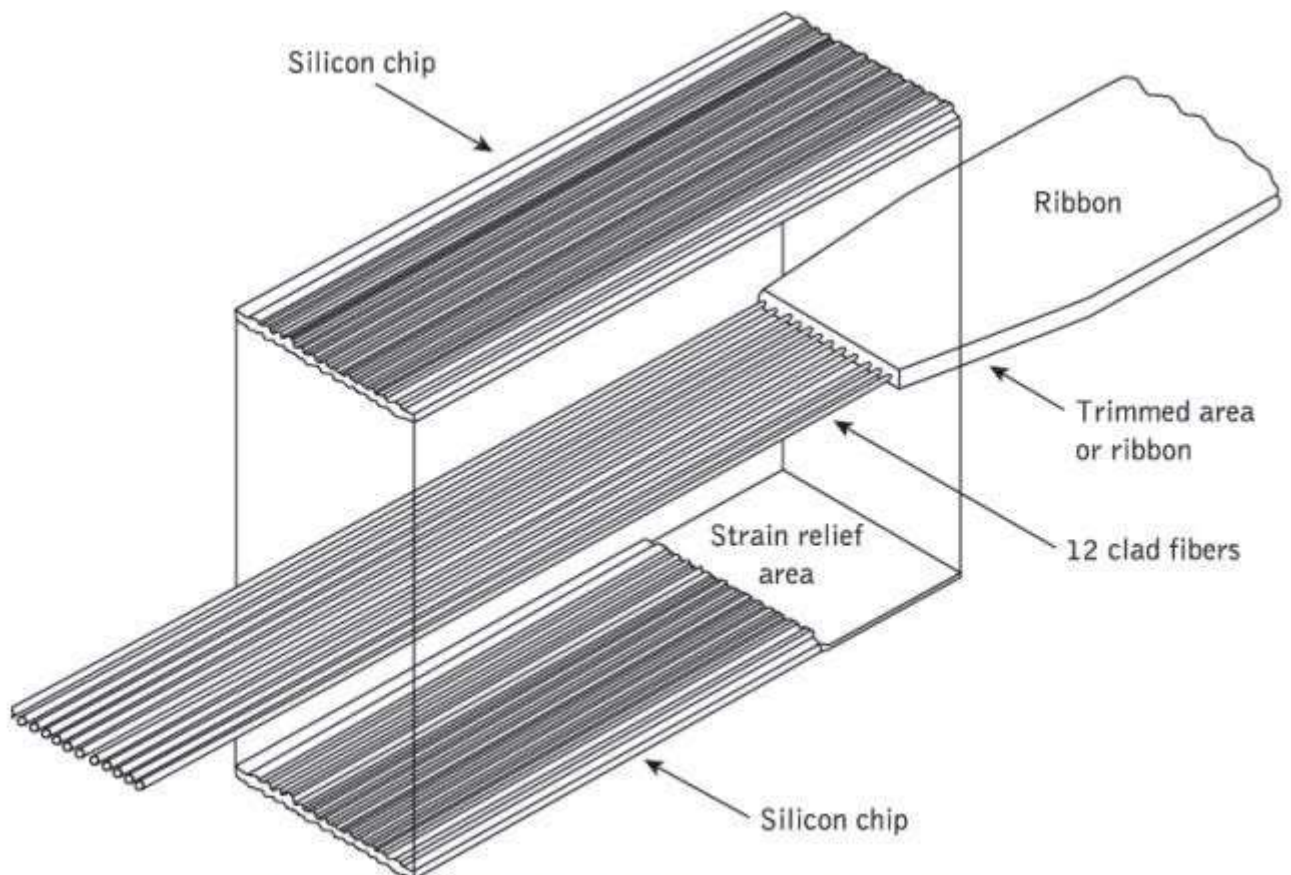


Figure 2.28 Multiple-fiber splicing using a silicon chip array

[Source: <http://img.brainkart.com>]

Nonlinear effects

Usually light waves or photons transmitted through a fiber have little interaction with each other, and are not changed by their passage through the fiber (except for absorption and scattering). There are exceptions, however, arising from the interactions between light waves and the material transmitting them, which can affect optical signals. These processes are normally referred to as nonlinear effects or phenomena because their strength typically depends on the square (or some higher power) of the optical intensity. Hence nonlinear effects are weak at low powers but they can become much stronger at high optical intensities. This situation can result either when the power is increased, or when it is concentrated in a small area such as the core of a single-mode optical fiber.

Although the nonlinear effects in optical fibers are small, they accumulate as light passes through many kilometers of single-mode fiber. The small core diameters, together with the long transmission distances that may be obtained with these fibers, have enabled the occurrence of nonlinear phenomena at power levels of a few milliwatts which are well within the capability of semiconductor lasers. Furthermore, the optical power levels become much larger when wavelength division multiplexing packs many signal channels into one single-mode fiber such that the overall power level is the summation of the individual channel optical powers. There are two broad categories of nonlinear effects that can be separated based on their characteristics: namely, scattering and Kerr effects.

Design Optimization Analysis

- RI profile
- Dispersion Calculation
- Cutoff wavelength
- Bending loss limitations

- RI profile: In design of single mode fiber dispersion behavior is a major one, it limit long distance and high speed of transmission
- For 1300nm,1550nm of single mode fiber the attenuation and dispersion effect
- For achieving maximum transmission distance, the dispersion should be null at the wavelength of minimum attenuation.
- By changing its refractive index core profile of fiber
 - a)1300nm optimized fiber
 - b)Dispersion shifted fiber
 - c)Dispersion flattened fiber
 - d)Large effective core area fiber

A) 1300nm Optimized Fiber

- most popularly used fiber
- 2-configuration-M-C fiber and D-C fiber
- Fibers that have a uniform refractive index throughout the cladding is called as M-C fiber or Matched-cladding fiber. MFD is $9.5\mu\text{m}$ & index difference is 0.35%
- Fiber that have the inner most cladding portion has low refractive index than outer cladding region is called D-C fiber or Dressed cladding fiber. MFD is $8.4\mu\text{m}$ & index difference $\Delta_1 = 0.25\%$, $\Delta_2 = 0.12\%$

B) Dispersion Shifted Fiber:

- here the material dispersion depends only on the composition of the material
- And waveguide dispersion is a function of the core radius, the refractive index difference is depends on shape of the RI profile

2-configuration: step index dispersion shifted fiber, Triangular dispersion shifted fiber

C) Dispersion Flattened Fiber

- Its more complex to design, it offers much broader of span wavelength.
- 2-configuration: Double clad profile fiber & Quadruple clad profile fiber.
- **Dispersion Calculation:** The total dispersion consists of material and waveguide dispersion effect, the inter modal dispersion is given as $D(\lambda)$ and broadening of optical pulse
- **Cutoff wavelength:** The amount of dispersion is caused by spectral width of fiber, is determined by fiber itself.
- $\lambda_c = 2\pi a/V_c(n_1^2 - n_2^2)^{1/2}$ where $V_c = 2.405$
- It decides radius of curvature

D) Large Effective Core Area Fibers:

- To reduce the non linearity large core area fiber is designed.
- $\lambda_c = 2\pi a/V_c(n_1^2 - n_2^2)^{1/2}$ where $V_c = 2.405$

Mode Coupling:

- After certain length due to mode coupling the pulse distortion increases rapidly
- By this energy from one mode is coupled to other mode.
- It occur due to
- Deviations of the fiber axis from straightness.
- Variations in the core diameter.
- Irregularities at core-cladding interface.
- Refractive index variations.
- Propagation characteristics of the fiber.
- Mode coupling is arise due to connectors, splices or other passive components in an optical link
- Due to this effect the individual mode do not propagate throughout length of the fiber.
- When the fiber is of good quality & not being bend large energy is transferred.

Bending Loss Limitations:

The micro bending and macro bending losses are significant in single mode fiber. These losses are function of MFD and Bend radius of curvature.

Modal Noise:

Is the effect of transmitted signal on optical channel. The speckle patterns observed in multimode fiber as fluctuations which have characteristic time longer than the resolution time of the detector, is known as modal (or) speckle noise.

- Multimode step index fiber
- Multimode graded index fiber

Group Delay:

In an optical fiber there are various modes present. Then the optical input, which is propagated along the fiber, will travel in various modes. Because of these modes the velocity of the signal will vary also there may be a delay in the optical signal of these various modes. This is called as the 'Group Delay'.

www.binils.com

Overall Fiber Dispersion

1. Multimode Fibers

The overall dispersion in multimode fibers comprises both chromatic and intermodal terms. The total rms pulse broadening σ_T is given by:

$$\sigma_T = (\sigma_c^2 + \sigma_m^2)^{1/2} \quad (2.44)$$

where σ_c is the intramodal or chromatic broadening and σ_m is the intermodal broadening caused by delay differences between the modes (i.e. σ_s for multimode step index fiber and σ_g for multimode graded index fiber). The chromatic term σ_c consists of pulse broadening due to both material and waveguide dispersion. However, since waveguide dispersion is generally negligible compared with material dispersion in multimode fibers, then $\sigma_c \approx \sigma_m$.

2. Single-Mode Fibers

The pulse broadening in single-mode fibers results almost entirely from chromatic or intramodal dispersion as only a single-mode is allowed to propagate.* Hence the bandwidth is limited by the finite spectral width of the source. Unlike the situation in multimode fibers, the mechanisms giving chromatic dispersion in single-mode fibers tend to be interrelated in a complex manner. The transit time or specific group delay σ_g for a light pulse propagating along a unit length of single-mode fiber may be given as:

$$\tau_g = \frac{1}{c} \frac{d\beta}{dk} \quad (2.45)$$

where c is the velocity of light in a vacuum, β is the propagation constant for a mode within the fiber core of refractive index n_1 and k is the propagation

constant for the mode in a vacuum. The total first-order dispersion parameter or the chromatic dispersion of a single-mode fiber, D_T , is given by the derivative of the specific group delay with respect to the vacuum wavelength λ as:

$$D_T = \frac{d\tau_g}{d\lambda} \quad (2.46)$$

In common with the material dispersion parameter it is usually expressed in units of ps nm⁻¹ km⁻¹. When the variable λ is replaced by ω , then the total dispersion parameter becomes:

$$D_T = -\frac{\omega}{\lambda} \frac{d\tau_g}{d\omega} = -\frac{\omega}{\lambda} \frac{d^2\beta}{d\omega^2} \quad (2.47)$$

The fiber exhibits intramodal dispersion when β varies nonlinearly with wavelength. β may be expressed in terms of the relative refractive index difference Δ and the normalized propagation constant b as

$$\beta = kn_1[1 - 2\Delta(1 - b)]^{1/2} \quad (2.48)$$

The rms pulse broadening caused by chromatic dispersion down a fiber of length L is given by the derivative of the group delay with respect to wavelength as

$$\begin{aligned} \text{Total rms pulse broadening} &= \sigma_\lambda L \left| \frac{d\tau_g}{d\lambda} \right| \\ &= \frac{\sigma_\lambda L 2\pi}{c\lambda^2} \frac{d^2\beta}{dk^2} \end{aligned} \quad (2.49)$$

where σ_λ is the source rms spectral linewidth centered at a wavelength λ .

When Eq. (2.44) is substituted into Eq. (2.45), detailed calculation of the first

and second derivatives with respect to k gives the dependence of the pulse broadening on the fiber material's properties and the normalized propagation constant b . This gives rise to three interrelated effects which involve complicated cross-product terms. However, the final expression may be separated into three composite dispersion components in such a way that one of the effects dominates each term. The dominating effects are as follows:

- ✓ The material dispersion parameter DM defined by $\lambda/c \left| \frac{d^2n}{d\lambda^2} \right|$ where $n = n_1$ or n_2 for the core or cladding respectively.
- ✓ The waveguide dispersion parameter DW , which may be obtained from Eq. (3.47) by substitution from Eq. (2.114) for τ_g , is defined as:

$$D_W = - \left(\frac{n_1 - n_2}{\lambda c} \right) V \frac{d^2(Vb)}{dV^2} \quad (2.50)$$

where V is the normalized frequency for the fiber. Since the normalized propagation constant b for a specific fiber is only dependent on V , then the normalized waveguide dispersion coefficient $V d^2(Vb)/dV^2$ also depends on V . This latter function is another universal parameter which plays a central role in the theory of singlemode fibers.

A profile dispersion parameter DP which is proportional to $d\Delta/d\lambda$

This situation is different from multimode fibers where the majority of modes propagate far from cutoff and hence most of the power is transmitted in the fiber core. In the multimode case the composite dispersion components may be simplified and separated into two chromatic terms which depend on either material or waveguide dispersion. Also, especially when considering step index multimode fibers, the effect of profile dispersion is negligible. Strictly speaking, in single-mode fiber with a power-law refractive index profile the composite

dispersion terms should be employed. Nevertheless, it is useful to consider the total first-order dispersion DT in a practical single-mode fiber as comprising:

$$D_T = D_M + D_W + D_P \quad (\text{ps nm}^{-1} \text{ km}^{-1}) \quad (2.51)$$

Polarization

Cylindrical optical fibers do not generally maintain the polarization state of the light input for more than a few meters, and hence for many applications involving optical fiber transmission some form of intensity modulation of the optical source is utilized. The optical signal is thus detected by a photodiode which is insensitive to optical polarization or phase of the lightwave within the fiber. Nevertheless, systems and applications have been investigated which could require the polarization states of the input light to be maintained over significant distances, and fibers have been designed for this purpose. These fibers are single mode and the maintenance of the polarization state is described in terms of a phenomenon known as fiber birefringence.

1. Fiber Birefringence

Single-mode fibers with nominal circular symmetry about the core axis allow the propagation of two nearly degenerate modes with orthogonal polarizations. They are therefore bimodal supporting HE_{x11} and HE_{y11} modes where the principal axes x and y are determined by the symmetry elements of the fiber cross section. Hence in an optical fiber with an ideal optically circularly symmetric core both polarization modes propagate with identical velocities. Manufactured optical fibers, however, exhibit some birefringence resulting from differences in the core geometry (i.e. ellipticity) resulting from variations in the internal and external stresses, and fiber bending. The fiber therefore behaves as a birefringent medium due to the difference in the

effective refractive indices, and hence phase velocities, for these two orthogonally polarized modes. The modes therefore have different propagation constants β_x and β_y which are dictated by the anisotropy of the fiber cross section. In this case β_x and β_y are the propagation constants for the slow mode and the fast mode respectively. When the fiber cross-section is independent of the fiber length L in the z direction, then the modal birefringence B_F for the fiber is given by:

$$B_F = \frac{(\beta_x - \beta_y)}{(2\pi/\lambda)} \quad (2.52)$$

Where λ is the optical wavelength. Light polarized along one of the principal axes will retain its polarization for all L . The difference in phase velocities causes the fiber to exhibit a linear retardation $\Phi(z)$ which depends on the fiber length L in the z direction and is given by:

$$\Phi(z) = (\beta_x - \beta_y)L \quad (2.53)$$

assuming that the phase coherence of the two mode components is maintained. The phase coherence of the two mode components is achieved when the delay between the two transit times is less than the coherence time of the source. the coherence time for the source is equal to the reciprocal of the uncorrelated source frequency width $(1/\delta f)$. It may be shown that birefringent coherence is maintained over a length of fiber L_{bc} (i.e. coherence length) when

$$L_{bc} \simeq \frac{c}{B_F \delta f} = \frac{\lambda^2}{B_F \delta \lambda} \quad (2.54)$$

where c is the velocity of light in a vacuum and $\delta \lambda$ is the source linewidth.

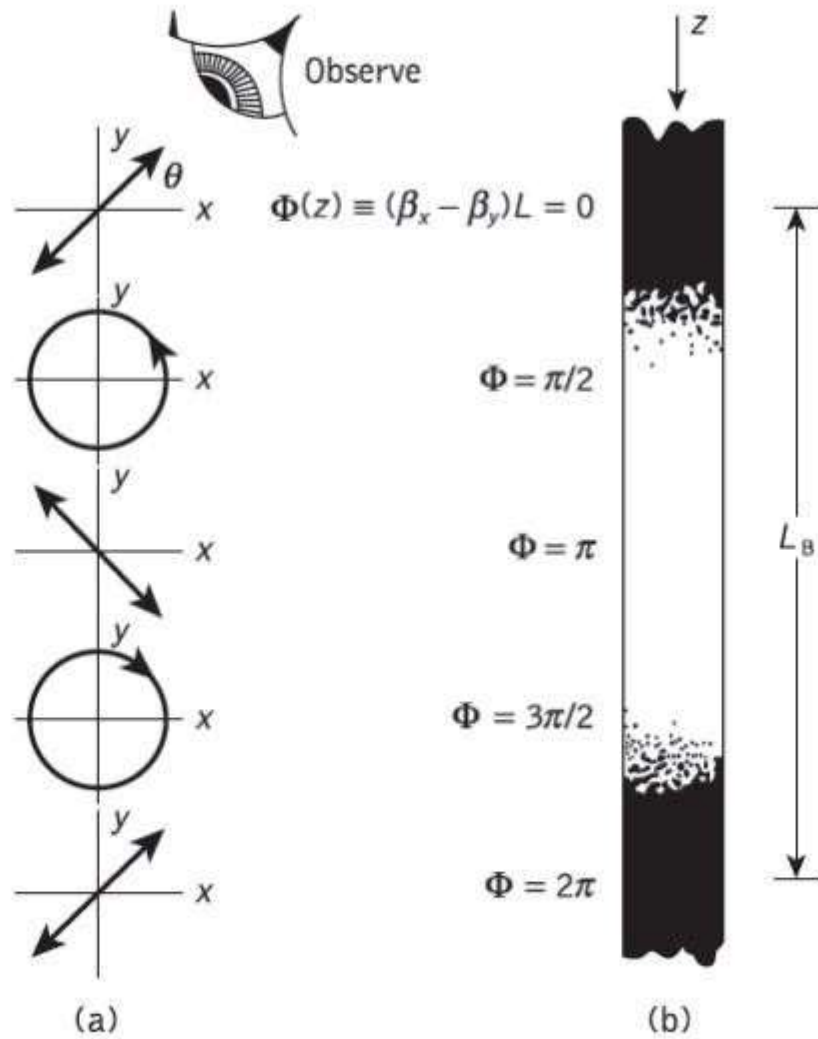


Figure 2.14 An illustration of the beat length in a single-mode optical fiber: (a) the polarization states against $\Phi(z)$; (b) the light intensity distribution over the beat length within the fiber

[Source: <http://img.brainkart.com>]

However, when phase coherence is maintained (i.e. over the coherence length) Eq. (2.58) leads to a polarization state which is generally elliptical but which varies periodically along the fiber. This situation is illustrated in Figure 2.14(a) where the incident linear polarization which is at 45° with respect to the x axis becomes circular polarization at $\Phi = \pi/2$ and linear again at $\Phi = \pi$. The process continues through another circular polarization at $\Phi = 3\pi/2$ before returning to the initial linear polarization at $\Phi = 2\pi$. The characteristic length L_B for this process corresponding to the propagation distance for which a 2π phase

difference accumulates between the two modes is known as the beat length. It is given by:

$$L_B = \frac{\lambda}{B_F} \quad (2.55)$$

Substituting for B_F from Eq. (2.47) gives:

$$L_B = \frac{2\pi}{(\beta_x - \beta_y)} \quad (2.56)$$

It may be noted that Eq. (2.56) may be obtained directly from Eq. (2.58) where:

$$\Phi(L_B) = (\beta_x - \beta_y)L_B = 2\pi \quad (2.57)$$

Typical single-mode fibers are found to have beat lengths of a few centimeters, and the effect may be observed directly within a fiber via Rayleigh scattering with use of a suitable visible source (e.g. He-Ne laser). It appears as a series of bright and dark bands with a period corresponding to the beat length, as shown in Figure 2.14.(b).

The modal birefringence B_F may be determined from these observations of beat length. In a nonperfect fiber various perturbations along the fiber length such as strain or variations in the fiber geometry and composition lead to coupling of energy from one polarization to the other. These perturbations are difficult to eradicate as they may easily occur in the fiber manufacture and cabling. The energy transfer is at a maximum when the perturbations have a period Λ , corresponding to the beat length, and defined by:

$$\Lambda = \frac{\lambda}{B_F} \quad (2.58)$$

However, the cross-polarizing effect may be minimized when the period of the perturbations is less than a cutoff period Λ_c (around 1 mm). Hence polarization-maintaining fibers may be designed by either:

(a) high (large) birefringence: the maximization of the fiber birefringence, may be achieved by reducing the beat length LB to around 1 mm or less

(b) low (small) birefringence: the minimization of the polarization coupling perturbations with a period of Λ . This may be achieved by increasing Λ_c giving a large beat length of around 50 m or more.

2. Polarization-Maintaining Fibers

Although the polarization state of the light arriving at a conventional photodetector is not distinguished and hence of little concern, it is of considerable importance in coherent lightwave systems in which the incident signal is superimposed on the field of a local oscillator. Moreover, interference and delay differences between the orthogonally polarized modes in birefringent fibers may cause polarization modal noise and PMD respectively. Finally, polarization is also of concern when a single-mode fiber is coupled to a modulator or other waveguide device that can require the light to be linearly polarized for efficient operation. Hence, there are several reasons why it may be desirable to use fibers that will permit light to pass through while retaining its state of polarization. Such polarization-maintaining (PM) fibers can be classified into two major groups: namely, high-birefringence (HB) and low-birefringence (LB) fibers.

The birefringence of conventional single-mode fibers is in the range $BF = 10^{-6}$ to 10^{-5} . An HB fiber requires $BF > 10^{-5}$ and a value better than 10^{-4} is a minimum for polarization maintenance. HB fibers can be separated into two types which are generally referred to as two-polarization fibers and single-

polarization fibers. In the latter case, in order to allow only one polarization mode to propagate through the fiber, a cutoff condition is imposed on the other mode by utilizing the difference in bending loss between the two polarization modes.

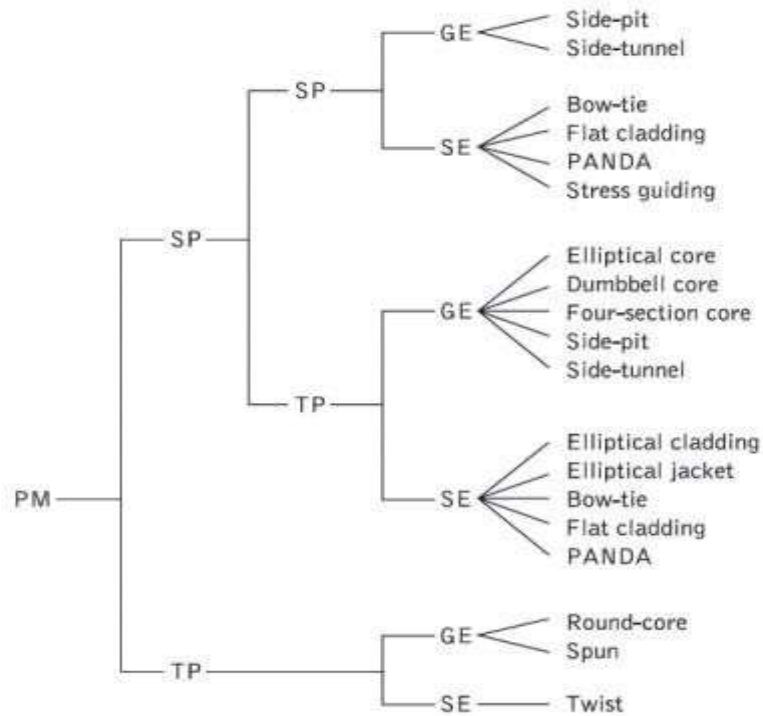


Figure 2.15 Polarization-maintaining fiber types classified from a linear polarization maintenance viewpoint. PM: polarization-maintaining, HB: high-birefringence, LB: low-birefringence, SP: single-polarization, TP: two-polarization, GE: geometrical effect, SE: stress effect

[Source: <http://img.brainkart.com>]

The various types of PM fiber, classified in terms of their linear polarization maintenance.